METHODS FOR IDENTIFICATION AND PRIORITIZATION OF STRESSORS AT IMPAIRED SITES

by

Elizabeth R. Nichols

A thesis submitted

in partial fulfillment of the requirements

for the degree of

Master of Science

Ecosystem Science and Management

in the University of Michigan

April 2023

Thesis Committee:

Professor G. Allen Burton, Chair
Associate Professor Andrew Gronewold

Table of Contents

Acknowledgements

First and foremost, I would like to thank Dr. Allen Burton for his invaluable guidance and mentorship throughout this entire process. In addition, I would like to thank Dr. Andrew Gronewold for his generous contributions as a committee member, Austin Crane for his limitless ingenuity and unrelenting support, members of the NIWC Pacific laboratory for their knowledge and warm welcome, Jacobs Engineering and Steve Brown for their knowledge and guidance, Bart Chadwick for his expertise and advice on the iTIE system, the Zak Lab and Rima Upchurch for advice and for allowing me to utilize their space, and Strategic Environmental Restoration and Demonstration Program for funding support.

Abstract

Aquatic ecosystems are often impacted by a multitude of stressors, many of which are introduced by a combination of anthropogenic activities such as agricultural development, urbanization, damming, and industrial discharge. Determining the primary stressors responsible for ecological impairments observed at a site where multiple stressors are present can be a complex and challenging task, however it is crucial for making informed management decisions. Improper diagnosis of an impaired system can lead to misguided attempts at remediation, which can be both time consuming and costly. This study focuses on the development, implementation, and evaluation of methodology that allows for differentiation between stressors, including optimization of *in situ* Toxicity Identification and Evaluation (iTIE) technology. This research focused on several tasks, including incorporation of a iTIE porewater sampling device, use of acetylcholinesterase activity to evaluate the feasibility of incorporating a chronic toxicity measure into the iTIE, capacity of different resins' ability to adsorb an organophosphate pesticide, and determining the role of dissolved oxygen and ammonia as stressors at a groundwater upwelling site. A combination of laboratory and field investigations were conducted, and the effectiveness of these methods were quantified through organism survival and enzyme activity. Overall, these approaches demonstrated the capacity to improve stressor identification in future contaminated site assessments.

In Situ Toxicity Identification Evaluation System

Background

The *in situ* Toxicity Identification Evaluation (iTIE) system was developed to address shortcomings of traditional laboratory TIEs through on site exposures of organisms to chemically fractionated surface/porewater (Burton et al., 2020; Burton & Nordstrom, 2004a; Burton & Nordstrom, 2004b; Steigmeyer et al., 2017). Identification of contaminants of concern (COCs) in the traditional TIE framework involves collection of samples at a site of interest and subsequently shipping the samples to a laboratory for chemical analysis, where they undergo chemical manipulations for isolation of targeted contaminants (US EPA, 2007; Ho et al., 2009). There are concerns surrounding the lack of realism associated with laboratory TIEs; samples are often stripped of factors that play an important role in the water chemistry of a site of interest, such as pH, microbial transformation rates, and chemical bioavailability (Burton et al., 2020). In addition, analysis is prone to sampling and instrument error, and can be a costly endeavor when a high volume of samples and/or multiple chemicals of interest are involved (Madrid et al., 2007; Blasco et al., 2009; Luo et al., 2021).

Laboratory toxicity testing faces similar concerns to chemical analysis of samples in terms of accuracy of site representation. Attempting to replicate the complexity of the natural environment within a controlled laboratory study can lead to disparities between lab results and field observations (Chapman, 2007). Factors such as temperature, food stress, and the presence of pathogens can result in the toxic effects of a particular contaminant being exacerbated in the field and thereby underestimated in a lab setting (Chapman, 1998). In addition, more than one COC can be present at a site, and proper evaluation of the toxicity of chemical mixtures using traditional laboratory methods requires extensive knowledge of the potential interactions between chemicals and the implications these interactions have for observed toxicity (Luo et al., 2021).

iTIE Concept and Design

As previously mentioned, the iTIE prototype addresses the uncertainties associated with laboratory testing by allowing for linkages between contaminant exposure and observed ecological impairments to be made within the field (Burton et al., 2020; Burton & Nordstrom, 2004a; Burton & Nordstrom, 2004b; Steigmeyer et al., 2017). The process by which this is achieved is depicted in Figure 1; peristaltic pumps pull up water from the source into acrylic, dual-chambered iTIE units, which is done at a low flow rate ($\leq$25 mL h^{-1}) to ensure resin adsorption capabilities are maximized (Burton et al., 2020). Water is pulled up through the selected resin before entering organism chambers, where organisms are exposed to the fractionated source water. Water then exits through the top outlet of the unit, being drawn into sample bottles at the same rate as it is being introduced to the iTIE unit. Various sizes of Nitex screens are placed between connections in the iTIE unit to prevent the resin particulates from entering organism chambers, as well as to prohibit organisms being pulled into sample bottles. Resins being sandwiched between glass wool also helps to prevent

particulates from exiting the resin chamber and serves the additional purpose of holding the resin in place to maximize contact with surface/porewater.

The use of multiple iTIE units with varied resins allows for visualization and quantification of the effects brought on by different contaminants within a site; resins such as Zeolite for removal of ammonia, Chelex for metals, Oasis HLB and Oasis WAX for per- and polyfluoroalkyl substances and activated carbon for a variety of compounds have been verified as candidates for use in the iTIE system. (Burton et al., 2020; Steigmeyer et al., 2017). Comparison of acute (mortality) and chronic (growth, reproduction, enzyme activity) endpoints of organisms exposed to water fractionated by various resins gives insight into the effects associated with different contaminants present at the site. The sample bottles can then be shipped off to a laboratory to be analyzed for verification of COC concentrations and resin efficiency.

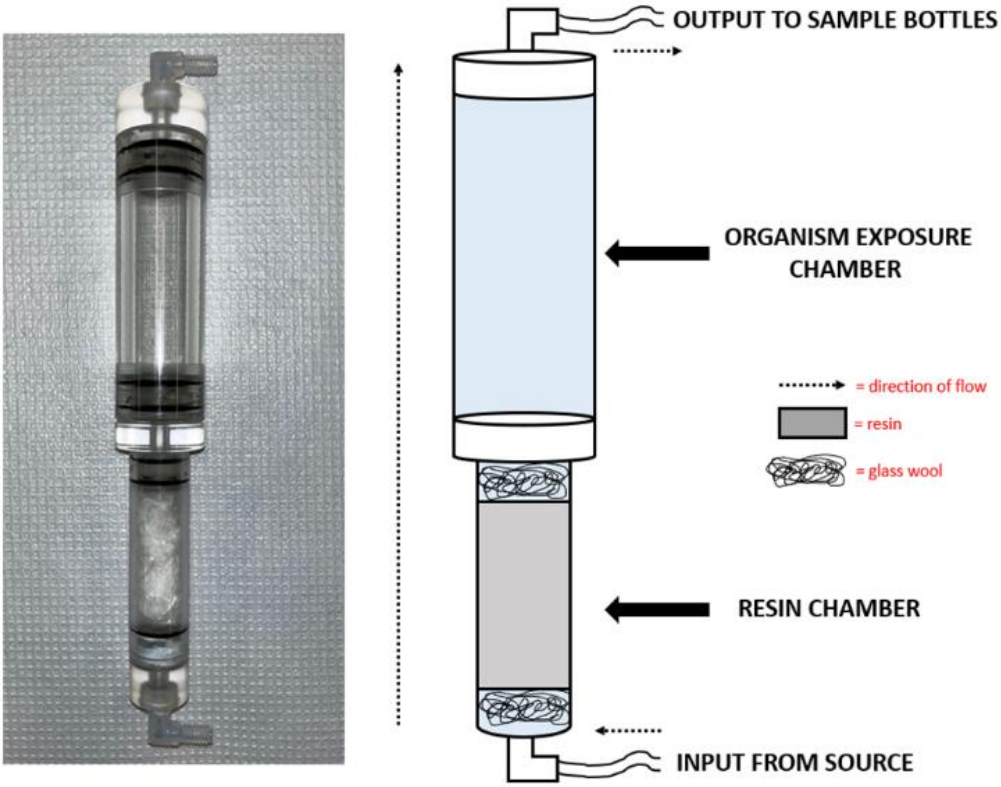

Figure 1: Depiction of dual-chambered iTIE unit and process of fractionation and subsequent exposure. Water is brought up from the source by peristaltic pumps, which then goes through the resin chamber containing resin sandwiched between glass wool. The resin selects for a contaminant of concern, and the fractionated water goes into organism chambers before exiting through outlet and into sample bottles.

Updated iTIE Prototype

The latest version of the iTIE prototype incorporates a proven porewater sampling device, referred to as the Trident. Sediment contamination is an important consideration in aquatic ecosystem assessment; contaminants that are not broken down, bioaccumulated, or otherwise diluted often accumulate in sediment, which then serves as a sink and source for contaminants (Kwok et al., 2014; Sojka & Jaskuła, 2022). Methods for assessing sediment contamination typically involve extraction of sediment cores which are then taken to a laboratory for subsequent analysis and toxicity testing (Burton & Johnston, 2010). Inclusion of a porewater sampling device into the iTIE system allows for improved linkage between exposure and effects of contaminants, providing improved realism that is not obtained in laboratory testing.

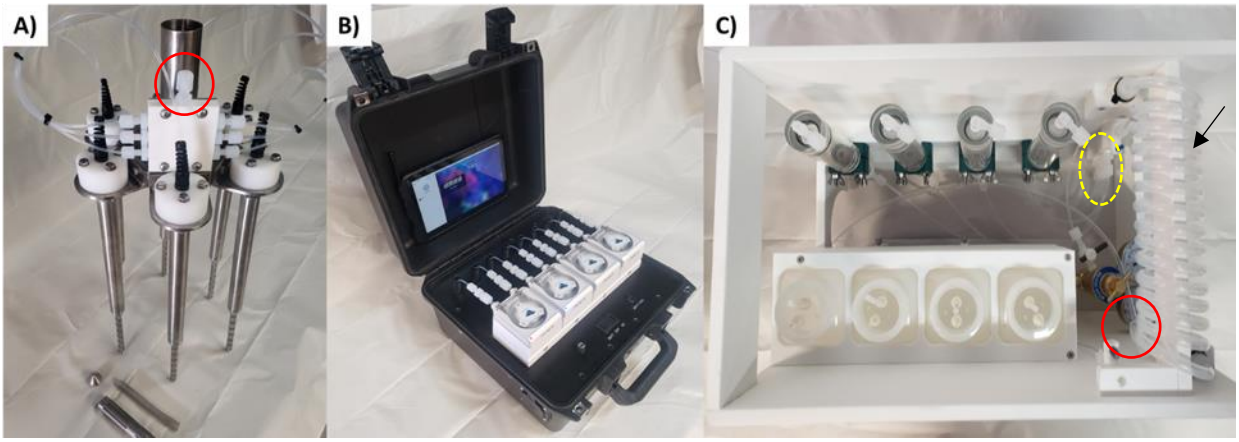

Figure 2: Components of the updated iTIE prototype. A) Trident porewater sampling device, with the red circle showing adapter where tubing responsible for bringing porewater into the iTIE rack is inserted. B) Versa Ecotech 4-Channel peristaltic pumps, controlled by app on tablet (pictured) through utilization of Bluetooth® technology. C) iTIE rack, which is typically held within a cooler to control temperature. Red solid circle denotes the entry point for surface/porewater tubing, black arrow points to oxygen coil, and yellow dashed circle shows location of manifold, where surface/porewater is diverted into separate iTIE units.

The updated iTIE prototype (Figure 2) includes the Trident (Figure 2A), Versa Ecotech 4-Channel peristaltic pumps (Figure 2B), and the iTIE rack (Figure 2C), which is typically kept within a cooler to control temperature. The iTIE rack includes iTIE units, sample bottles, and an oxygen canister and coil. The oxygen canister serves as a source for the oxygen coil, where O_2 is diffused into porewater through a gas-permeable Teflon tubing coil. The addition of the oxygen coil is to account for porewater being oxygen deficient, and oxygenation of porewater ensures organisms mortality will not be attributed to low dissolved oxygen (DO) concentrations. The concept of the updated prototype is similar to the iTIE system, with

minor changes. An overview of the updated iTIE protocol for sampling of shallow porewater is depicted in Figure 3, and described in greater detail in Appendix A.

In summary, the Trident probes are inserted ~2-3 inches into the sediment, and the Versa pump tubing attached to the top of the iTIE units are responsible for slowly pulling up shallow porewater into the oxygen coil. After the water has gone through the oxygen coil, it enters the manifold where it is evenly divided between the 4 iTIE units. It then goes through the same process as previously mentioned; water is fractionated by resins before entering organism chambers and exiting through the top of the units into 500 mL HDPE sample bottles. To refine the operation and functionality of this system, multiple deployments were carried out at both marine and freshwater sites varying in depth.

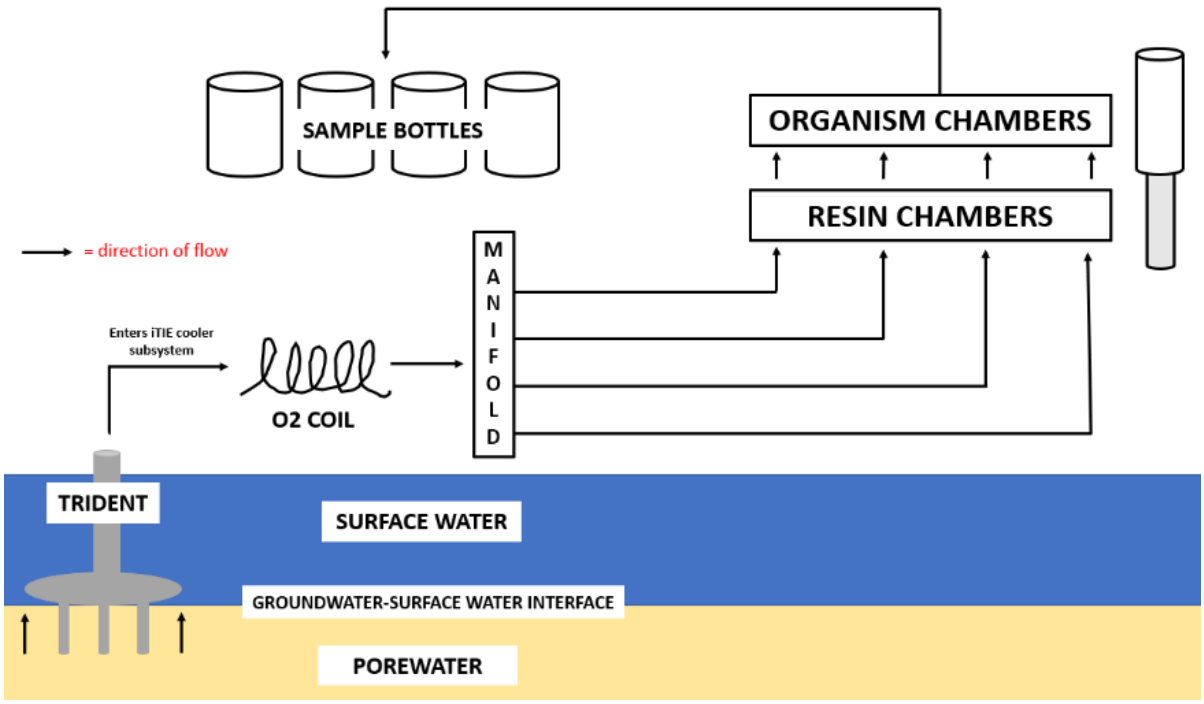

Figure 3: Overview of iTIE system for sampling shallow porewater. In the interest of clarity, Versa pumps were omitted from the diagram, but are responsible for the movement of water throughout the system.

Testing and Field Deployment of iTIE Prototype

Oxygen Coil Testing

To quantify the effectiveness of the oxygen coil, tests were executed comparing the DO of an oxygen deficient source to DO of the water after it had passed through the oxygen coil. Source water was bubbled with nitrogen to lower DO content and was subsequently pulled through the oxygen coil at a slow rate to imitate the speed at which exposures would be conducted. After the water had passed through the coil, flow rate was increased to empty the coil and retrieve a sample of ~50mL. Initial tests were carried out in absence of oxygen diffusion to determine the level of aeration achieved through the coil alone. DO was measured using a handheld DO meter, and the results of oxygen tests are displayed in Figure 4. DO increased by an average of 2.4 mg/L (± 0.60 (s.d)) when source water was run through the coil in the absence of oxygen and increased by an average of 8.1 mg/L (± 1.9 (s.d)) when the oxygen system was turned on. These results verify the oxygen coil's capability to aerate anoxic porewater, allowing for shallow porewater to be incorporated into the iTIE system without concerns of adverse effects on organism survival.

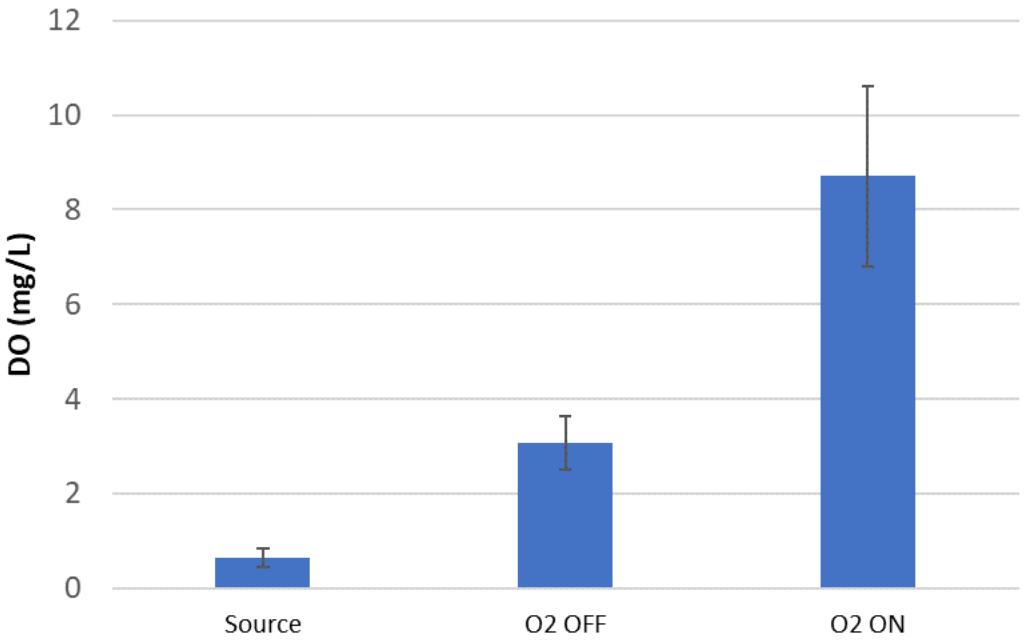

Figure 4: Results of oxygen coil tests, with "Source" being average DO (mg/L) of oxygen deficient water used for tests, O2 OFF representing DO concentrations after the source water had been through the oxygen coil without the oxygen system turned on, and O2 ON is DO after oxygen coil with oxygen system on. Error bars represent standard deviation.

Initial Deployment (May 2022)

The initial deployment of the updated iTIE system was conducted off a pier located on NIWC Pacific property in San Diego, California. The purpose of this deployment was for field validation of the Trident porewater sampler addition to the iTIE system, therefore resins and organisms were not included.

Preparation for the run included cleaning the Trident and adjusting the stopper plate (Figure 5A) to the desired depth of sampling. Metal mesh screens were then added over each of the probes, followed by a second metal filter. The space in between the metal mesh screen and the filter was filled with glass beads, and metal caps were added to the end of each probe. The purpose of these steps was to prevent sediment from entering and clogging the Trident. Versa pumps were attached to respective iTIE units; tubing responsible for pulling water in was attached to the top outlet of the iTIE units, and tubing pushing water out was attached to sample bottles (Figure 5B). The bottom inlets of each iTIE unit were connected to manifold tubing (Figure 2C), and iTIE units were primed with surface water prior to the initiation of the run. One end of a ¼" tube, cut to the approximate length of the distance between the Trident and the iTIE cooler, was inserted into the adapter located on the base of Trident (Figure 2A), and the other end was attached to the adapter in the iTIE cooler (Figure 2C).

The Trident was deployed to a depth of ~20 feet, which was done using a diver-less deployment system. The diver-less deployment system involved the attachment of multiple poles that were used to lower the Trident and lodge it into the sediment, and the extra poles were then released with a push-pin release mechanism and brought back to the surface. The Trident was secured to the dock with a rope for retrieval after the completion of the run. After deployment of the Trident, the oxygen system was primed with porewater, using a Masterflex® Portable Sampler to bring up porewater from the Trident to the oxygen coil (Figure 5C). This porewater was diverted away from the iTIE units using a T-valve, and exited through an auxiliary tube, preventing the initial influx of sediment from going into the units and allowing for the functionality of the oxygen system to be tested. Once the oxygen coil was primed and confirmed to be operational, the run was initiated for 24 hours at a combined flow rate of 80mL/hour (20 mL/hour per unit).

After completion of the run, the Versa pumps were stopped, and the portable sampler was used to expel water remaining in the oxygen coil, which was subsequently tested to ensure DO had remained at an acceptable level. The oxygen system was then turned off, and the portable sampler pulled additional porewater, which was also tested for DO for further verification of the oxygen coil effectiveness. DO for oxygenated water was 9.8 mg/L, which was higher than the DO of non-oxygenated porewater (4.8 mg/L). Sample bottle volumes were checked, and ranged from 453-530 mL, confirming Versa pumps were pumping within a reasonable range of the targeted flow rate. The difference in volumes between sample bottles did not demonstrate a clear pattern, and suggested further calibration of Versa pumps was needed to prevent this issue. Overall, the initial run showed promising results for the integration of the Trident into the iTIE system.

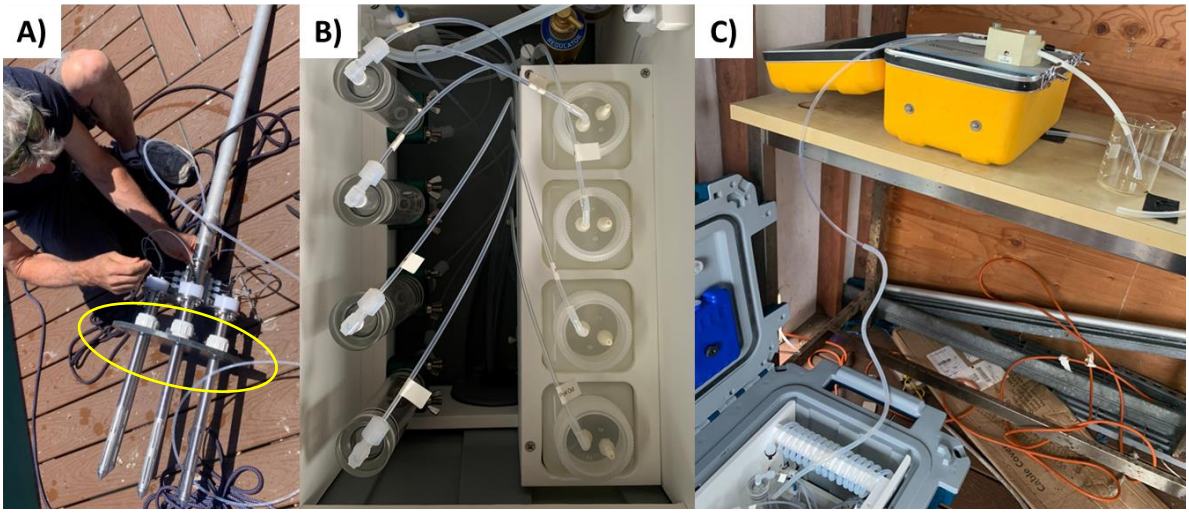

Figure 5: Images from the initial deployment of the updated iTIE prototype. A) Preparation of the Trident, with yellow circle showing location of stopper plate. B) Versa pump tubing connected to iTIE units and sample bottles C) Portable sampler used to prime oxygen coil.

Laboratory Testing with *Americamysis bahia* (September 2022)

A test using water spiked with copper was conducted to establish a standard operating procedure for the addition of resins and organisms. This was done in a controlled laboratory setting and did not include the Trident, as it was centered around refining the methods for resin and organism addition with the updated iTIE rack system to streamline these steps for future Trident tests.

Filtered seawater with a salinity of 34 ppt was spiked with Cu solution (1 ppm) to evaluate the efficiency of resins. Two-day old mysid shrimp (*Americamysis bahia)* cultured by Aquatic Biosystems (Fort Collins, CO) were used. Mysid shrimp 96-hour LC50s for Cu ranges from 0.141-0.181 mg/L (Rosen et al., 2009), meaning mortality would likely be observed in organism chambers containing resins that did not target this compound. The resins selected included Oasis HLB, Chelex, activated carbon, and glass wool as a control. Five grams of each resin was used.

Initial concerns involved the correct time to add resins because flow rates used to prime Versa pump tubing resulted in the resins being disturbed and entering the organism chamber. This led to the decision that resins should be wetted before addition to resin chambers, and resin addition should occur after Versa pumps are primed. Furthermore, organism chambers should be manually filled with water to prevent resin disturbance. Another problem encountered was the use of powdered activated carbon (PAC); the fine grain size of PAC led to particles escaping the resin chamber, as the Nitex filter was unable to contain the resin. Reducing the mesh size of the filter raised concerns for clogging and flow resistance, and the decision to switch to activated carbon filtered through a 90µm sieve was made. The addition

of 10 mysids to each unit was the final step in this process, and the run was initiated at a flow rate of 20 mL/hr. Ten mysids were a laboratory control.

The test was terminated after 18 hours, and organisms counted for survival (Fig 6). Overall, Chelex had the highest survival as expected due to it being the only resin capable of sorbing copper. Complete mortality was observed within GAC, which later studies suggested was due to low DO. The control had 100% survival, which was not observed in any of the iTIE units. However, evidence for cannibalism within the iTIE units was noted, suggesting mysid shrimp may not be the ideal candidate for iTIE exposures. The volumes within each sample bottle were all around 350 mL, indicating pumps were calibrated correctly.

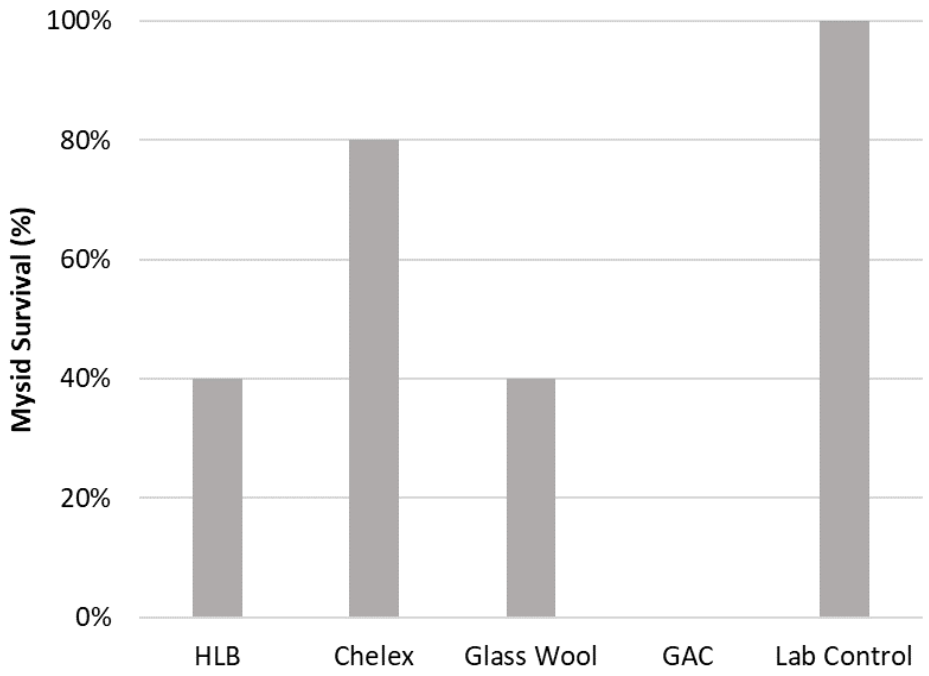

Figure 6: Survival (%) for mysid shrimp in chambers with respective resins after 18-hour exposure to 1ppm copper spiked FSW.

Paleta Creek Deployment (September 2022)

The first full field deployment involving the Trident, resins, and organisms took place at Paleta Creek in San Diego, CA. Paleta Creek flows into Naval Base San Diego, and the presence of multiple contaminants has been documented at this site, with an emphasis on pyrethroid pesticides (Hayman et al., 2020). The primary goal of this deployment was to provide field validation for the updated iTIE prototype, with the secondary goal of assessing toxicity at Paleta Creek.

Preparation for deployment was identical to the protocol established during the initial trial off the pier at NIWC Pacific, with the addition of resins and organisms. Mysid shrimp were the organisms chosen for this study, and HLB, Chelex, granular activated carbon (GAC) and a glass wool control (5 grams each) were once again used as resins. Resins were added after the system was primed, and iTIE units were filled manually with culture control water, with the addition of organisms being the final step.

Multiple issues were encountered throughout the duration of the exposure. Before the addition of organisms and resins, a leak in the oxygen system was detected. The oxygen canister was then replaced; however, a faulty DO meter gave little to no insight into whether this issue was fixed. Once resins and organisms were added and the run was initiated, porewater being pulled up from the Trident began to retreat down to the source. This was attributed to the surface of the water being too far below the iTIE cooler subsystem; the low flow rate required for maximizing resin adsorption (20 mL/hour, combined flow rate of 100 mL/hour) was unable to overcome gravity. To counteract this issue, the Masterflex® Portable Sampler was used to bring water up from the Trident into a secondary container, and water was pumped from this container into the iTIE cooler subsystem. The higher flow rate of the portable sampler was able to overcome gravity, and the container was flushed every 30 minutes for 10 minutes at a time to ensure fresh porewater was being introduced.

While the issue of gravity was addressed, organism mortality was observed within a few hours from the initiation of the run. Within 8 hours, there was complete mortality across all 4 of the iTIE units, and the run was terminated. The faulty DO meter was replaced and DO measurements of the water held within the iTIE units were recorded. HLB, GAC, and glass wool all had reasonably high DO concentrations, falling within the range of 6-8 mg/L. However, GAC DO was around 2 mg/L, which is below the EPA recommendation of 4.0 mg/L for mysids (US EPA, 2002). Nevertheless, the cause of mysid mortality could not be attributed to DO alone, due to the higher DO content observed in iTIE units where mortality occurred. The change in temperature is another factor could have played a role in organism stress, with temperature at the initiation of the run being 28℃, compared to 21℃ at the time that the run was terminated. While the cooler the iTIE rack is encased in helps to maintain a constant temperature, the myriad of issues experienced during the run resulted in the cooler being opened and closed many times during troubleshooting attempts.

Fleming Creek Deployment (November 2022)

A field deployment was conducted in Fleming Creek, Ann Arbor to investigate the performance of the updated iTIE prototype in a shallow, freshwater creek scenario. One-day old *Daphnia magna* and 7–14-day old *Hyalella azteca* from UM cultures were used in this deployment. Preparation for the test included overnight acclimation of organisms from culture room temperature (21℃) to expected field temperature (16℃). Organisms were kept in a cooler for transportation to the field to ensure minimal temperature fluctuation. Resins included Chelex, granular activated carbon (GAC), Zeolite, and a glass wool control (5

grams each). Preparation steps followed the same guidelines as described by the previous deployments, as well as in Appendix A.

Gravity issues were once again encountered during the preparation phase. The portable sampler was unable to draw water up from the Trident while positioned at the backend of the oxygen coil, which is how it was situated in previous runs. The solution was to instead put the portable sampler at the front end of the iTIE cooler subsystem (Figure 7A), allowing it to push water through the coil as opposed to pull. The exposure was conducted for a 24-hour exposure, with pumps running at 20 mL/hour.

After test initiation, water in the source tube began to backflush. The system was examined for leaks, and a leak was found at the source tube adapter in the iTIE cooler subsystem. This leak was addressed by wrapping plumbers' tape around the inside of the adapter, thereby tightening the fit (Figure 7B). After the leak was fixed, the porewater was able to overcome gravity and flow into the iTIE units.

Upon return to the site at the end of the 24 hours, a large bubble had formed in the oxygen coil (Figure 7C). This bubble had prevented the expected volume of water from flowing through to iTIE units, resulting in sample bottles not receiving the expected volume (Figure 8A). The iTIE system relies on the maintenance of pressure, and the introduction of air leads to a vacuum being formed in the oxygen coil. Bubbles in the oxygen coil led to less water being pulled through to iTIE units, and when the manifold is not saturated with water gravity will pull water down to the bottom of the manifold, resulting in unit 4 receiving the highest volume, which steadily decreases with respective unit position (Figure 8B).

DO concentrations showed the oxygen system was operational; porewater DO was 3.68 mg/L, compared to DO within chambers ranging from 9.55 – 9.88 mg/L. Organism survival ranged from 70-100% for *D. magna* and 80-100% for *H. azteca*, however survival rates cannot be accurately compared across units due to the dramatic differences in the volume of porewater organisms were exposed to.

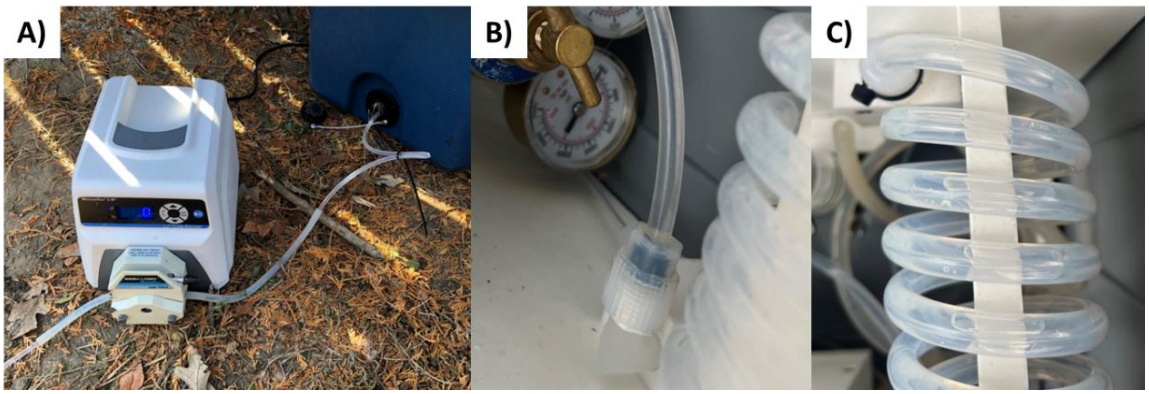

Figure 7: A) Peristaltic pump positioned at front of iTIE subsystem. B) Plumbers tape on inside of source water tube adapter to prevent leak. C) Bubbles in oxygen coil

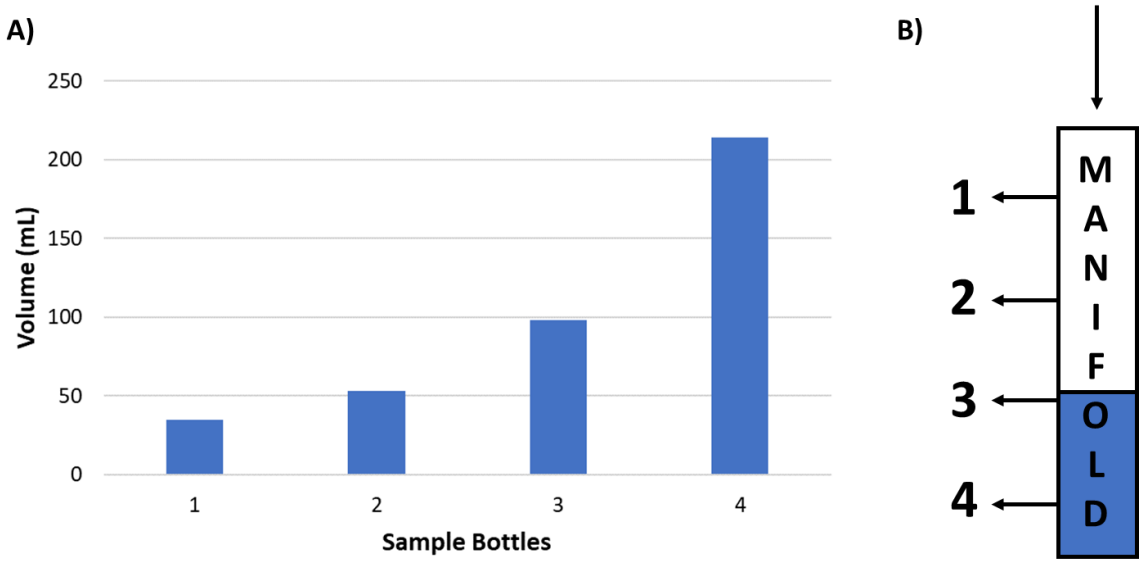

Figure 8: A) Volume (mL) of sample bottles after 24-hour Fleming Creek exposure. B) Diagram showing uneven water distribution to iTIE units and sample bottles when manifold is not saturated.

Future Directions

The primary issues needing to be addressed are the inability for the low flow rate required for maximum resin adsorption to overcome gravity, and the introduction of air resulting in a vacuum forming within the oxygen coil. The component of gravity will be prevalent at most sites, especially those with fluctuating water levels, and a completely airtight system is unrealistic. Therefore, these problems will need to be addressed to increase reliability and expand the sites at which this technology can be deployed.

The addition of the peristaltic pump on the front end of the system was proposed as a permanent solution to be included for the duration of the exposure, with the pump running at a slightly higher speed than the Versa Pumps and overflow being diverted out of the system. This solution has undergone preliminary testing in the laboratory, and promising results were achieved, with bubbles in the DO coil being minimized and sample bottles having uniform volume. Continued development of this proposed solution will likely lead to integration of the pump into the system, allowing for the negation of issues associated with gravity.

Additional testing includes quantification of Trident drawdown in various sediment types to understand how long the Trident can be deployed before surface water is pulled into the sampler. The evaluation of resins is another ongoing project for further optimization of the iTIE system, with additional / more specific resins allowing for isolation of more contaminants.

AChE Activity as Short-term Chronic Toxicity Endpoint for the iTIE and Optimizing iTIE Resin Selection for Chlorpyrifos

Introduction

Pesticides are frequently infiltrating waterways through agricultural runoff and spray-drift, which poses a threat to the survival of organisms that inhabit these contaminated ecosystems (Schulz, 2004). Aquatic invertebrates are of particular concern, as they are often more vulnerable to the effects of pesticides due to sharing a similar morphology to typical target pesticide species (Bartlett et al., 2016). The heightened sensitivity of aquatic invertebrates to pesticides can lead to high rates of mortality being observed at extremely low concentrations (Maggio et al., 2021; Rasmussen et al., 2013).

Chlorpyrifos is particularly well known for lethal effects observed at low doses, with *Hyalella azteca* demonstrating a 10-d LC50 of 0.0086 µg/L and 48-hour LC50 of 0.1 µg/L (Phipp et al., 1995; Moore et al., 1998). This highly toxic pesticide is classified as an organophosphate, which is a commonly used class of pesticides that also includes malathion, diazinon, and parathion (Ganie et al., 2022). Organophosphates are grouped by their mechanism of lethality, which is inducing neurotoxicity through the inhibition of acetylcholinesterase, an enzyme that aids in the degradation of the neurotransmitter acetylthiocholine (Julien et al., 2008). Acetylcholinesterase (AChE) activity of organisms can be established through bioassays, and this has been utilized as a chronic endpoint for quantification of organophosphate exposure for aquatic species (Naddy et al., 2000; Day & Scott, 1990; Laetz et al., 2020).

The main goals of this study were to 1) establish a protocol allowing for integration of AChE activity as a short-term chronic toxicity endpoint for future iTIE deployments and 2) use AChE to evaluate resin effectiveness for absorption of chlorpyrifos. Incorporating AChE activity into the iTIE protocol would improve the overall robustness of the system by providing insight into the presence of contaminants below the levels required to induce mortality within a 24–48-hour period. On the other hand, if concentrations of chlorpyrifos are at levels where lethality can be observed, employment of a resin with the capability of isolating this toxic insecticide would provide more clarity concerning the primary stressors at that site. These objectives were accomplished through laboratory iTIE runs with chlorpyrifos-spiked water that organisms were exposed to after the water was fractionated by various resins, and the effectiveness of the resins were determined through comparison of AChE activity of the exposed organisms.

Methods

Test Organisms

Freshwater benthic macroinvertebrate *H. azteca* were obtained from an existing laboratory mass culture at the University of Michigan. This culture was kept within a 5-gal aquarium tank filled halfway with ion-enriched water and was fed 2 rabbit pellets on M and F. Adult *H.*

azteca were utilized in this study to maximize tissue for AChE analysis. Adults were collected by filtering through a 600 µm mesh sieve (Plomp et al., 2020), and groups of 10 each were transferred into 30 mL centrifuge tubes prior to exposure.

Resins and Chemicals

Resins tested in this study included Oasis HLB (Waters™), Amberlyst-15 (Sigma Aldrich), activated carbon (Marineland), and C18 SPE (Waters™) (Figure 9). Oasis HLB and C18 are both designed for solid phase extraction, with Oasis HLB being preferred for the extraction of polar compounds (Dias & Poole, 2002), and C18 using hydrophobic interactions to adsorb non-polar compounds. Chlorpyrifos is relatively non-polar, however, HLB was still considered as a candidate as it also has non-polar compound adsorption capabilities. Activated carbon, as previously mentioned, can adsorb a wide range of compounds. Amberlyst-15 was chosen due to its demonstrated ability to adsorb malathion, an organophosphate sharing structural similarity to chlorpyrifos (Dias & Poole, 2002).

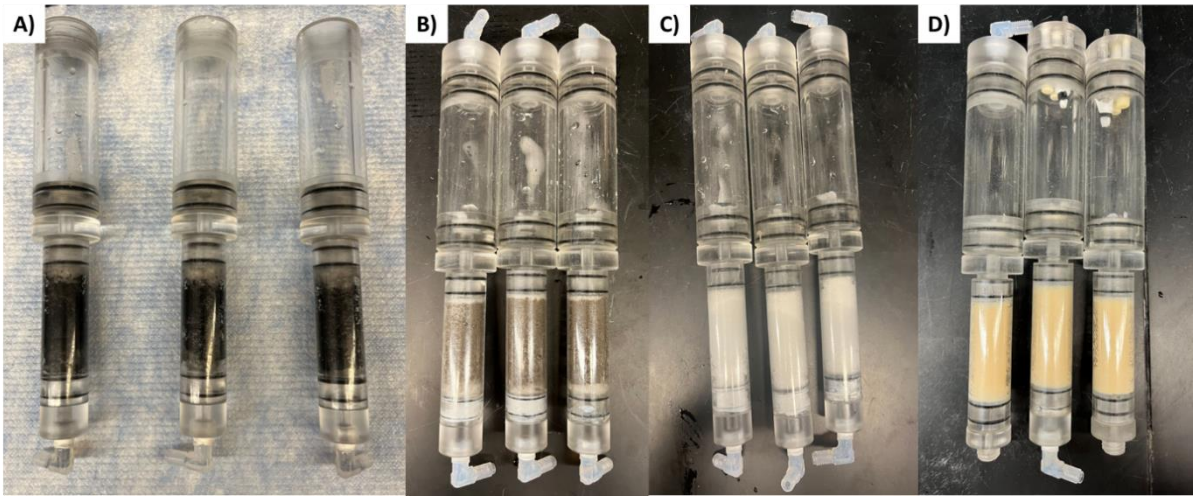

Figure 9: Resins tested for adsorption of chlorpyrifos. A) Activated carbon B) Amberlyst-15 C) C18 D) Oasis HLB

Chlorpyrifos and chemicals used for AChE analysis were obtained from Sigma Aldrich. 10 mg of chlorpyrifos was mixed with 100 mL of acetone to yield a stock solution of 0.1 µg/mL, which kept in an amber bottle stored in the refrigerator to prevent degradation. The quality control enzyme standard was prepared daily at a concentration of 0.2 units/mL of electric eel acetylcholinesterase and homogenizing buffer. The homogenizing buffer (pH=7.4) consisted of 1% v/v Triton X-100/Tris buffer (0.05 M), with the tris buffer being prepared at pH 8. Ellman's reagent was prepared by diluting 0.025 g of Ellman's powder with homogenizing buffer and adjusted the pH of the solution to 7.4. Acetylthiocholine iodide (0.156 M) and bicinchoninic acid working reagent were both prepared daily. Bicinchoninic acid working reagent was prepared by making a 50:1 volumetric ratio of bicinchoninic acid solution with

4% (w/v) copper (II) sulfate pentahydrate. BSA protein standards were made at concentrations of 0 µg/mL, 200 µg/mL, 400 µg/mL, 600 µg/mL, 800 µg/mL, and 1000 µg/mL by dilution of bovine serum albumin with homogenizing buffer.

Chlorpyrifos Exposure

To establish a streamlined protocol for exposure, preliminary tests with granular activated carbon (GAC) were conducted due to its availability, low cost, and ability to adsorb a wide range of contaminants (Burton et al., 2020). The results from the GAC trials led to the following exposure protocol to be established.

A total of 3 chlorpyrifos exposure runs were conducted, and each run was associated with a different resin. 6 iTIE units were used per run, with 3 treatment iTIE units containing 5 grams of resin (sandwiched between glass wool) and 3 control units containing glass wool. Prior to the initiation of the exposure, Versa pump tubing was purged with ethanol, followed by a rinse with Liquinox and Milli-Q. iTIE units and sample bottles were rinsed with Liquinox and soaked in a 10% HCL solution. Quality control samples of 500 mL were taken to establish if any chlorpyrifos was leaching off equipment. Versa pump tubing was then primed with ion-enriched water (IEW).

A chlorpyrifos-spiked water solution was prepared by adding 60 µL of 0.1 µg/mL stock solution to 6000 mL of IEW, for a final concentration of 1.0 µg/L. This solution was kept within a 2.5-gallon aquarium tank, rinsed with ethanol in between runs, and iTIE units were placed in this aquarium for the duration of the exposure (Figure 10A).

Resins were conditioned with either Milli-Q (HLB, Amberlyst-15) or methanol (C18) before being added into iTIE units. Once resins were added, the units and sample bottles were attached to their respective Versa pump tubing. Chambers were filled with IEW, and 10 adult *H. azteca* were added to each unit (Figure 10B). The run was then initiated, with each Versa pump running at 25 mL/hour for a 24-hour exposure. Water quality parameters (DO, temperature, pH) were recorded for both the IEW and chlorpyrifos-spiked water.

At the end of the exposure, *H. azteca* were removed from iTIE units and counted. These organisms were then divided into respective centrifuge tubes, with each centrifuge tube sample containing 5 organisms (2 samples of 5 organisms each per iTIE unit). The exception for this was cases where mortality was observed, resulting in the remaining organisms within an iTIE unit being split between two centrifuge tubes. Centrifuge tubes were place in a -80°C freezer until AChE analysis. Water quality parameters were recorded for both water within the iTIE unit and sample bottles, and volume of sample bottles was also recorded. Sample bottle volume was then transferred into amber bottles to be stored in the refrigerator until analysis. Additionally, a 500 mL sample of the remaining volume of chlorpyrifos-spiked water was transferred into an amber bottle for analysis. The samples were shipped off within 24 hours of the exposure to Eurofins, Canton for analysis of chlorpyrifos.

An additional 24-hour test was conducted in the absence of chlorpyrifos in order to obtain baseline levels of AChE activity. The baseline run followed the aforementioned steps, with

the exception of chlorpyrifos being added to the water, and all 6 iTIE units contained glass wool.

Figure 10: A) Setup for chlorpyrifos exposure, with aquarium tank containing water spiked with chlorpyrifos to a concentration of 1.0 µg/L B) Addition of organisms to iTIE units.

AChE Activity Quantification

The following protocol for the acetylcholinesterase analysis utilized for quantifying toxicity was adopted from Bartlett et al., 2016.

Hyalella azteca were thawed on ice before being homogenized in 500µL of homogenizing buffer and spun down in a centrifuge for 10 minutes. The supernatant from centrifuged samples was then transferred into a new centrifuge tube to be used for analysis.

Acetylcholinesterase determination was carried out by addition of 40µL of homogenizing buffer, sample supernatant, or quality control standard into separate wells of a 96-well round-bottom plate, with samples being run in triplicate (Figure 11A). This was followed by the addition of 250µL of 5,5'-dithiobis{2-nitrobenzoic acid]) to each well, and the reaction was initiated by adding 10 µL of acetylthiocholine iodide (Ellman et al., 1961). After addition of acetylthiocholine iodide, absorbances were immediately read on a microplate spectrometer every 2 minutes for 30 minutes at 405nm. It is worth noting that the quality control sample was degraded due to exposure to suboptimal temperature during trial runs and could not be included in AChE analysis of samples examined for this study. However, the quality control absorbance was within expected bounds before degradation occurred, and the same reagents were used for exposure run AChE analysis (Appendix C).

Protein concentration was measured using a BSA standard curve. This was done by adding 25µL of supernatant in triplicate and 25µL of each of the BSA protein standards. 200µL of bicinchoninic acid solution was then added to each well, and the plate was incubated at 25°C for 2 hours before reading absorbances at 562 nm (Figure 11B). The standard curve was then used to calculate protein concentrations of the sample supernatant. Specific activity for AChE was then calculated using the equation shown in Figure 12.

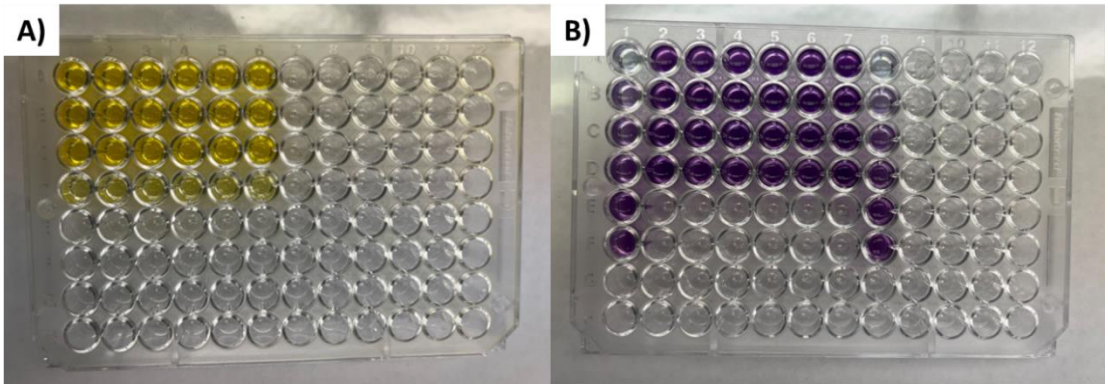

Figure 11: A) AChE activity plate. B) BSA protein plate after 2-hour incubation.

$$Specific\ activity = (A \times Vol_R \times 1000) / (E \times PL \times Vol_H \times PR)$$

Figure 12: Equation used to calculate specific activity for AChE (in µmol/min/g protein), where A= change in absorbance/min, Vol_R= reaction volume (0.3 mL), E=extinction coefficient for 5,5'-dithiobis{2-nitrobenzoic acid]) ($1.36 \times 10^4\ M^{-1}\ cm^{-1}$), PL= pathlength (0.875 cm), Vol_H= sample volume (0.04 mL), and PR= protein in the homogenate calculated from standard curve (mg/mL).

Statistical Analysis

Average specific activity for *H. azteca* for resin and glass wool chambers in chlorpyrifos exposures were divided by average baseline activity to express specific activity as a percentage of baseline. Standard deviation was calculated through propagation of error.

Student's T-tests were used to compare average specific activity of *H. azteca* associated with resin and glass wool iTIE units in chlorpyrifos exposures to average specific activity of baseline organisms. A p-value of ≤0.05 was used to determine statistical significance.

Results & Discussion

Granular Activated Carbon

As previously mentioned, GAC was used in preliminary trials to establish standard operating procedure for chlorpyrifos exposure. These tests were originally carried out using the iTIE rack, which was changed due to the rack being able to only contain 4 units at a time. All units were removed from the rack and transferred into the aquarium tank to keep treatment consistent across all units.

During the tests in which the iTIE rack was used, increased mortality was observed in units containing GAC, with units having survival rates of 0%. Further investigation showed DO

levels reaching levels of concern that likely resulted in observed mortality (Figure 13). However, not all units shared the same low levels of DO. The unit containing GAC that was positioned further down on the manifold had the lowest DO and DO increased with positioning on the manifold. This is related to the trend concerning uneven water distribution and sample bottle volume observed during Fleming creek deployment (Figure 8); while gravity pulls down water to the bottom of the manifold, air can escape at the top of the manifold, resulting in unit 1 receiving more oxygen. Although the manifold likely plays a role in observed DO levels, glass wool was positioned furthest down on the manifold and demonstrated higher DO levels than GAC counterparts, suggesting GAC contributed to lower DO content.

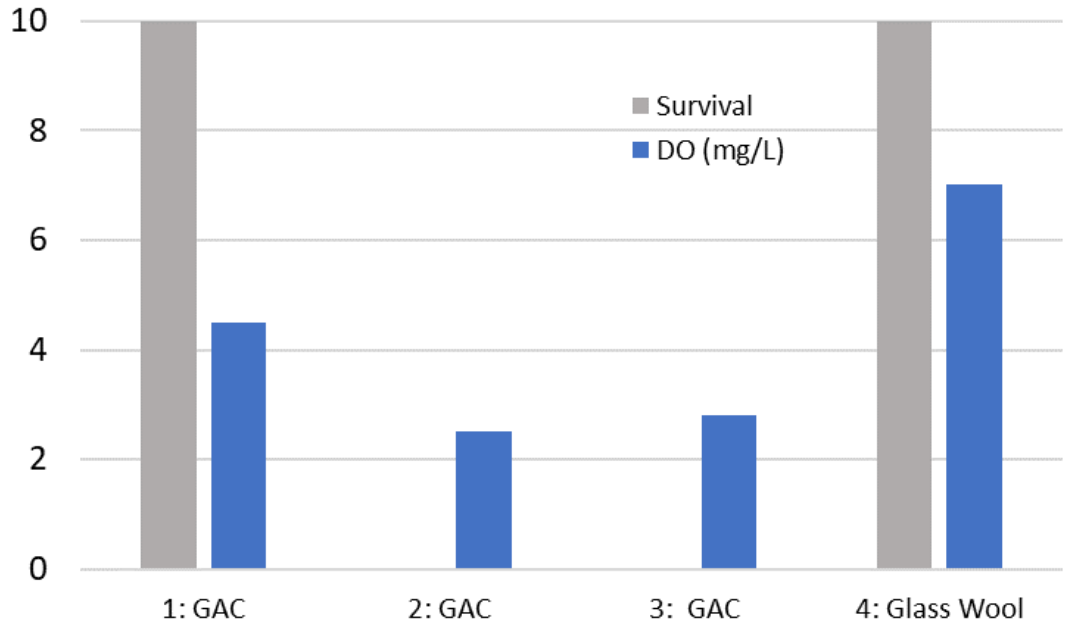

Figure 13: Survival (maximum survival = 10) and observed DO content within respective resin chambers. Number in front of resin chamber denotes position on manifold, with 1 being at the top and 4 at the bottom.

While previous iTIE prototype exposures were successful when using GAC (Burton et al., 2020), the closed nature of the updated iTIE prototype can result in uneven distribution of oxygen and limits the amount of oxygen that can enter the system. This appears to be less of a concern in runs where the oxygen coil is in operation (Fleming Creek), however, use of future exposures GAC should take DO concerns into account to avoid falsely attributing mortality to a stressor present at the site.

Amberlyst-15

Amberlyst-15 also encountered issues with regards to adverse impacts on organism survival. Less than 2 hours into the run, mortality within iTIE units containing Amberlyst was observed, and complete mortality in these units occurred within 5 hours. The run was terminated, and water quality measurements revealed pH levels ranging from 2.27 – 2.32. Glass wool pH ranged from 7.6-7.7, and no mortality occurred within these units. This provides evidence supporting acidic conditions within Amberlyst units being attributed to the resin, ultimately leading to the complete mortality of *H. azteca*. The low pH in these chambers can likely be explained by Amberlyst-15 being a hydrogen form resin, and the exchange of water led to an excess of hydrogen ions entering the organism chamber, lowering the pH.

C18 & Oasis HLB

AChE activity of organisms in units with C18 (Figure 14A) and Oasis HLB (Figure 14B) alludes to both resins having the capacity for adsorption of chlorpyrifos. Average specific activity for organisms in glass wool chambers for the C18 run was 70% (± 16% (s.d.)) of baseline activity; AChE activity is considered to be inhibited when it is ≤80% of baseline activity, proving organisms within glass wool chambers were exposed to chlorpyrifos (Bartlett et al., 2016). In addition, average glass wool specific activity was proven to significantly differ from mean baseline activity (p =0.001). On the other hand, C18 average specific activity was 94% (± 24% (s.d.)) of baseline activity and did not significantly differ from average baseline activity (p = 0.47).

Organisms in chambers where water was fractionated by HLB also had a higher average specific activity as a percent of baseline (98% ± 19% (s.d.)) than organisms in glass wool (80% ± 22% (s.d.)). Mean specific activity for HLB was not significantly different from mean baseline activity (p = 0.82), but a significant difference was observed for glass wool (p = 0.03).

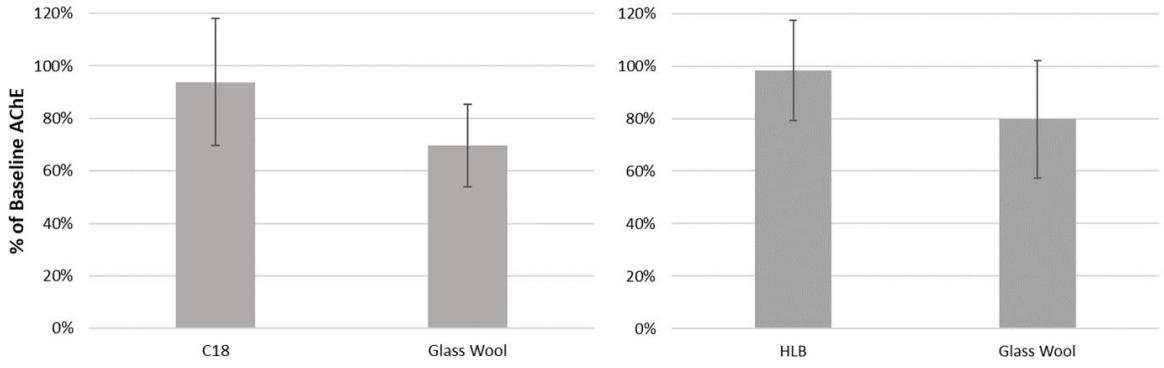

Figure 14: A) Average specific activity (expressed as % of baseline) for C18 run B) Average specific activity for HLB run. Error bars represent standard deviation, and asterisk denotes significant difference between treatment and baseline activity ($p \leq 0.05$).

Laboratory Analysis

Analysis of samples fell below Eurofins' minimum detection limit of 0.50 µg/L, therefore no chlorpyrifos was detected in any of the samples. However, laboratory quality control (QC) samples ran alongside samples showed losses of up to 12.0 ug/L when comparing QC sample concentration to concentration detected, suggesting that chlorpyrifos was likely present within the samples shipped off, but was unable to be detected by the instruments. This highlights the need for specialty laboratories when analyzing compounds with concentrations in the parts per billion (ug/L) range.

Conclusions

While adsorption capabilities were unable to be confirmed due to the inadequate detection limit by Eurofins, AChE specific activity suggests C18 and HLB were successful in removal of chlorpyrifos. In addition, methods for quantification of AChE activity as a chronic toxicity endpoint were successfully established for use in future iTIE deployments.

This study highlighted the need to consider the role resins can play in alteration of critical water quality parameters, which can lead to increased stress and mortality. Failure to account for effects of resins on organisms can lead to falsely attributing these adverse impacts to site conditions, as previously mentioned.

Future resin optimization should also consider cost, availability, and specificity of resins. Expensive resins that are not widely available are unrealistic for use in the iTIE system, and increased specificity allows for the effects of targeted contaminants to be isolated. While Oasis HLB and C18 demonstrated successful adsorption of chlorpyrifos, these resins have been proven to adsorb other contaminants that could be also be present at a site (Burton et al., 2020). This lack of specificity has implications for the accuracy of linkage between exposure and effects; improved organism health within chambers containing these resins cannot be directly attributed to a single contaminant, and definitive conclusions cannot be made without laboratory analysis of sample bottle concentrations. While the aforementioned factors are important to consider, finding a resin that meets these criteria can be a difficult task, and resins lacking one of these qualities can still be utilized in future iTIE deployments.

.

Weight-of-Evidence Evaluation of Potential Groundwater Upwelling Site in Ludington, MI

The following study is to be viewed independently from the previous sections, as it is written for journal submission. To reflect this, figure numbers were restarted.

Introduction

The multitude of stressors present within aquatic systems, often introduced by anthropogenic activity, has emphasized the importance of stressor characterization within these complex, dynamic environments. In the presence of multiple stressors, attribution of impairments to their respective stressor can be a challenging process (Fanelli et al., 2022). Establishing a causal link between stressors and observed ecological impairments is a critical component of contaminated site assessment; formulation of plans for remediation and restoration are dependent on proper diagnosis of the problem (Burton & Johnston, 2010). Efforts to improve site conditions are often costly and time consuming (Bernhardt et al., 2005), and confidence in the effectiveness of their outcomes can be improved through ensuring the primary sources of impairment are addressed (Suter et al., 2002; Palmer et al., 2010).

Toxic contaminants being introduced into waterways and sediments is a well-documented stressor category within risk assessments (Fanelli et al., 2022). A common approach in assessment of sites suspected to be compromised by the presence of one or more pollutants is comparing detected concentrations of samples to established sediment and water quality guidelines (Altenburger et al., 2019., Blasco et al., 2009, Burton et al., 2010). Determining concentrations of contaminants of concern (COCs) is oftentimes integral to understanding potential causes of impairment, however, this particular methodology has several disadvantages (Michalaki et al., 2022). Proper sampling design is crucial for reducing uncertainty in reported detections; selection of sampling sites that are misrepresentative of site conditions as well as low sampling frequency can lead to inaccurate predictions of biological impacts (Madrid et al., 2007). While obtaining a large, representative set of samples is ideal, especially for sites with temporal and spatial heterogeneity, this is not always possible due to transportation and analytical costs (Blasco et al., 2009; Madrid et al., 2007). Even in scenarios where large sample sizes can be obtained, the manipulation of samples during analysis can reduce accuracy (Burton et al., 2020), and the presence of chemical mixtures adds additional challenges regarding analysis and estimation of exposure effects (Luo et al., 2022).

Aside from the uncertainties associated with chemical monitoring, chemistry-driven strategies comparing sample concentrations to water/sediment quality guidelines can fail to consider the prevalence of other stressors within a system, leading to inaccurate conclusions concerning stressor causality. US EPA's Stressor Identification Guidance Document lists several stressors that would likely remain undetected during assessment of site chemistry,

including siltation, altered flows, invasive species, and loss of habitat (US EPA, 2000a). The application of biological monitoring, as opposed to chemical monitoring, can be a useful tool for quantifying the extent to which various stressors have impacted organisms at a particular site (Govenor et al., 2017). This process involves the comparison of the overall health and composition of communities at a site of concern to communities at a nearby, minimally disturbed site sharing similar characteristics, otherwise known as a reference site (US EPA, 2011). Benthic macroinvertebrates are prime candidates for bioassessments due to their sensitivity to pollution as well as the existence of well-developed indices that relate the composition of these communities to overall water quality (Fierro et al., 2017). Employment of this method allows for more insight into ecological impairments than provided by site chemistry, however it does not directly identify the stressors responsible for the observed effects.

This study utilizes a weight-of-evidence (WOE) approach to characterize the effects of contaminated groundwater exfiltration (upwelling), from an unlined wastewater settling basin, on surrounding benthic macroinvertebrate communities. WOE approaches integrate several lines of evidence (LOE) such as site chemistry, biological monitoring, and toxicology to reduce the uncertainty associated with using only one of the aforementioned methods and increase the accuracy of stressor causality (Burton et al., 2002). The site investigation was conducted over the period of several years, and the following LOE were included: 1) Physicochemical characterization of near-surface porewaters and near-bottom surface waters; 2) Benthic invertebrate community indices using grab samples and reciprocal transplant methods; 3) Laboratory worst-case scenario toxicity testing; 4) *In situ* toxicity testing; 5) Diurnal monitoring of dissolved oxygen (DO); and 6) Manipulation of DO in limnocorrals with concurrent in situ toxicity testing. Lines-of-evidence were established through adaptive management; each line was developed after analysis of the results from the prior investigation. Initial examination of the site led to the discovery of dramatic diurnal dissolved oxygen fluctuations as well as elevated concentrations of contaminants of potential concern (COPCs), with a particular emphasis on ammonia. This led to the integration of the final two LOE (Phase 4), with the goal of differentiating between the effects of natural and anthropogenic stressors, which will be the focus of this study.

Methods

Site Description

Relative locations of the site of interest (E-11) and reference site (Ref-E) investigated in this study are depicted in (Figure 1). Site E-11 is located along the northwest side of South Pond, bordering Pere Marquette Lake in Ludington, MI. Previous phases have shown E-11 to have elevated COPC concentrations in groundwater and sediment-surface interface porewater, as well as low diversity in benthic macroinvertebrate. In addition, there has been evidence of pronounced diurnal DO fluctuations within this area, which led to E-11 being chosen for the current phase. Ref-E was chosen as a reference site due to its similarities in habitat conditions

and lack of groundwater-surface water interface releases, as established through previous phases.

Figure 1: Location of sites utilized in this study, with Reference D/E being referred to as "Ref-E" and Station E as "E-11".

Limnocorral Design

Four cylindrical limnocorrals (LCs) were used in this study (Figure 2), with each LC consisting of two rings of one-half-inch polyvinyl chloride (PVC) forming the top and bottom edges of the cylinder, connected by density polyethylene (HDPE) plastic sheeting forming the cylinder's walls. PVC rings had an approximate radius of 1.6 feet, and the height of each LC was around 3 feet. LCs were oriented vertically, and both the top and bottom circular faces were left open. The seams of the plastic sheeting were sealed with waterproof tape to prevent water from flowing through horizontally. Additional plastic sheeting was attached to the bottom PVC ring with waterproof tape to form a skirt.

Each LC was secured at each station using four steel fence posts, which were placed on the interior of the plastic sheeting and hammered several inches into the sediment. The top PVC ring of each LC was zip-tied to the fence stakes, holding the plastic sheeting taut and keeping the LC up several inches above the water's surface. Weighted gravel socks and cinder blocks were placed on the base of each skirt, further anchoring the LC in place, and preventing the flow of surface water under the bottom ring.

Three LC treatment "scenarios" were established at each of the two stations (Figure 3). For the first LC scenario (LCA), an LC was installed and four Marina Aquarium Air Pumps with

accompanying 4-inch air stone bars were employed continuously through the course of the experiment to provide aeration of the interior water column. For the second LC scenario (LCNA), an LC was installed, but the interior water column was not aerated. For the third LC scenario (LCO), no LC was installed, and the area was open to natural lake conditions.

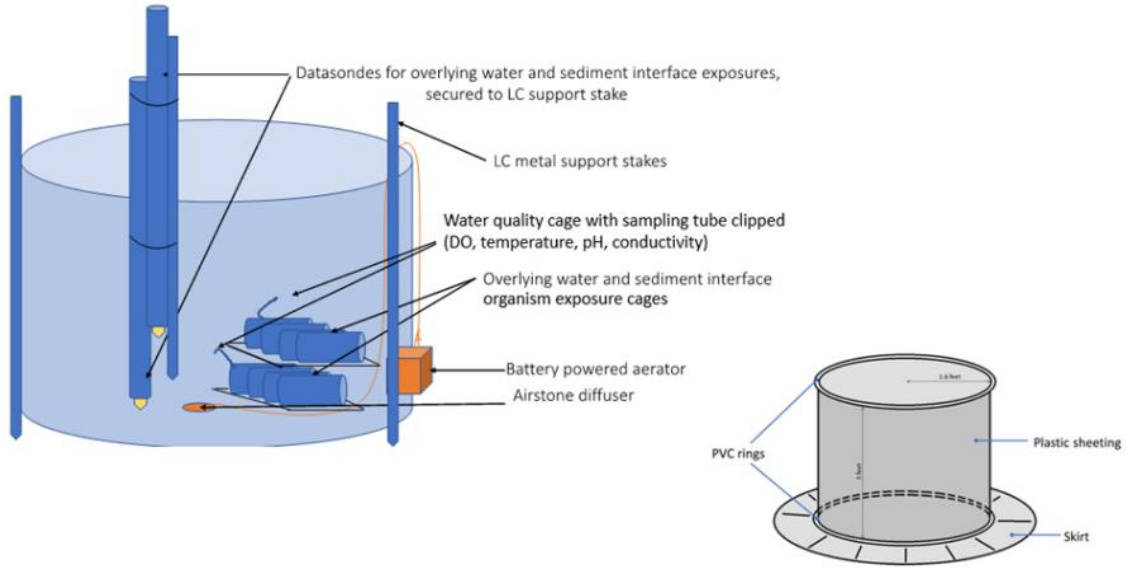

Figure 2: Limnocorral experimental design.

Figure 3: Limnocorral set up at E-11 (left) and Ref-E (right). The stake in the middle with signage was the location of the no limnocorral treatment (LCO).

In Situ Chamber Design

The design and arrangement of *in situ* organism exposure chambers is pictured in Figure 4 and described in greater detail in Burton et al. (2005). Each exposure chamber was

constructed from a cellulose acetate butyrate cylinder, 12.7 cm long with an inner diameter of 6.67 cm, and sealed on each end with polyethylene cap. The curved surface of the chamber had two rectangular windows (4 x 8 cm) cut opposite of one another and covered in 74-80 µm mesh.

Each LC scenario had 8 chambers total, which were secured attached to a rack. Four replicate test chambers were secured on top of the rack, oriented with both windows exposed to overlying column water (OW), and four replicate test chambers were secured to the bottom, oriented with one window against the surficial sediment (SS). In addition, two test chambers without organisms were included for water sampling, one with OW orientation and one with SS orientation. These water quality (WQ) chambers each contained a port with a piece of tygon tubing, to allow for water sampling by syringe. The positioning of these chambers within limnocorrals is pictured in Figure 2.

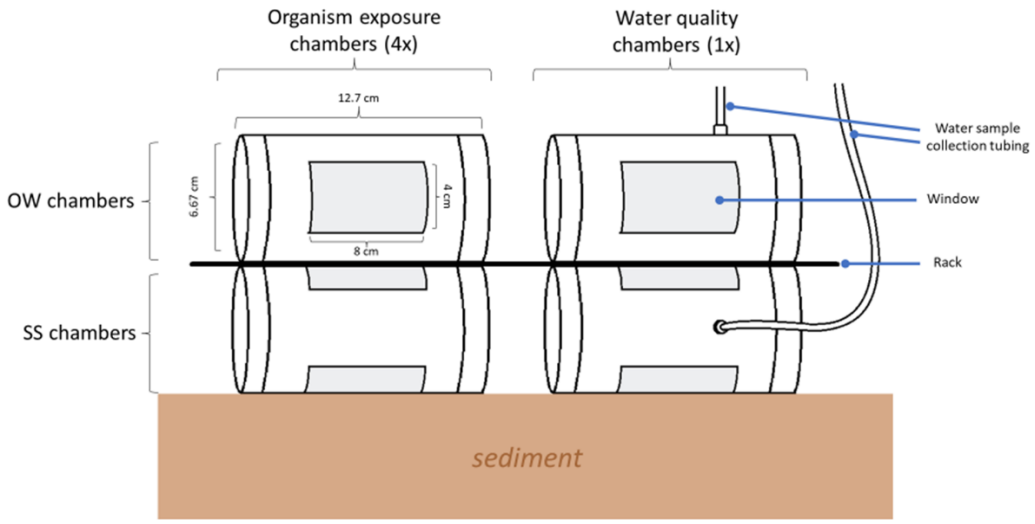

Figure 4: Design and arrangement of *in situ* exposure chambers.

Test Organisms

The organisms utilized in the *in situ* exposure were juvenile *H. azteca* (7-14 day old) cultured by Aquatic Biosystems in Fort Collins, CO. *H. azteca* were shipped overnight and arrived in Ann Arbor, MI on July 30, 2022. The organisms were shipped in a 4-liter Cubitainer® inside of climate-controlled packaging. Upon arrival, the container was aerated and 50% of the water volume was replaced with ion-enriched water. The Cubitainer® included wheatgrass and brine shrimp flakes to serve as sources of food. The organisms were transported to

Ludington, MI the following day and were kept in the Cubitainer® placed inside of a cooler that was continuously monitored to ensure minimal fluctuation in temperature. Upon arrival, the container was aerated overnight by tygon tubing attached to a Marina Aquarium Air Pump. The morning of deployment (August 1) the organisms were sorted into 53 sets of 10 organisms each (8 sets of 10 per LC scenario, 5 sets for travel controls), with each set kept in a Fisherbrand™ 50 milliliter (mL) polypropylene centrifuge tube filled with ion-enriched water (IEW). All 53 centrifuge tubes were kept within coolers for transportation to the field stations.

To determine the role transportation (Ann Arbor to Ludington, between field stations) played in the observed mortality rates of organisms utilized in the *in situ* exposures, 5 sets (50 organisms total) of travel controls were included. The travel control *H. azteca* were exposed to the same conditions as the *in situ H. azteca*, but were not deployed into chambers. Instead, upon return from field stations, the travel control organisms were placed in a climate-controlled setting and transferred into containers with aerated IEW and monitored. On the last day of the *in situ* exposure (August 5), surviving travel control *H. azteca* were counted to establish a baseline rate of mortality due to travel-related stress.

Field Deployment

The chambers were deployed on August 1 (Day 0) and retrieved on August 5 (Day 4), 2022 for a 4-day *in situ* exposure. On Day 0, small coolers were filled with surface water from each station, and chambers were submerged within the cooler and filled with water. While submerged, 10 *H. azteca* were loaded into each OW and SS chamber. There were 10 chambers in total (4 OW, 4 SS and 1 WQ for each treatment). The chambers were fastened to a metal rack using bungee cords and gently deployed to their respective LC scenario (1 rack per LC scenario per station for 6 total) and secured in place with rocks and small stakes.

Daily sampling activities were conducted from August 2 (Day 1) to August 5 (Day 4), 2022 for each LC scenario, with the exception of station REF-E on Day 2 (August 3) due to weather related issues. Following daily sampling, the LC sides were dropped to allow for the exchange of new lake water and subsequently refastened to the steel fence posts.

On the final day of deployment (August 5, 2022), chambers were retrieved from each LC treatment. This was accomplished by submerging a small cooler in water and transferring the rack of chambers into the submerged cooler to avoid any water from being lost from the chambers. Chambers were then removed individually and rinsed into counting trays with spray bottles containing surface water. The number of surviving *H. azteca* within each chamber was recorded.

Water Quality Monitoring Sampling

At each station, a pair of AT600 water quality data logging sondes were deployed for each LC scenario (Figure 2). Each sonde pair was installed with sensors positioned at a depth that corresponded to the *in situ* exposure treatment chambers (SS and OW). For this positioning, sondes were affixed to the steel stakes using plastic zip ties. The sonde sensors deployed in

parallel with the SS chambers were set as close to the surface sediment as possible, without being submerged in the soft substrate. The sonde sensors deployed in parallel with the OW chambers were positioned approximately 4 inches above the sediment surface.

Daily chamber water samples were taken by attaching a BD Luer-Lok™ syringe to the end of the tubing on the WQ chambers and pulling up to retrieve a 30 mL sample from both OW and SS chambers. Water quality measurements were taken for each sample, including DO, temperature, conductivity, and pH. The following instruments were used to record these measurements: YSI ProODO dissolved oxygen meter, YSI Conductivity/Temp handheld meter, and Orion Star™ A121 Portable pH meter. In addition to chamber water samples, airstone sampling techniques were employed to retrieve daily pore water samples from surficial sediments in each LC scenario. Four-inch ALEGI airstone bars with Tygon tubing attached were completely inserted into the sediment, and a BD Luer-Lok™ syringe was attached to the end of the tubing to withdraw by suction, ~50 mL of pore water. Samples for measurement of chlorides and TDS were sampling at the same depth as the in line with SS chamber and pulled to the surface using tubing and a peristaltic pump. All of the aforementioned samples were transferred into bottles and shipped cold by overnight express for analyses.

Airstone and chamber samples were submitted to Eurofins Laboratory in Lancaster, Pennsylvania (Eurofins Lancaster) for analysis of ammonia by U.S. Environmental Protection Agency (EPA) Method 350.1. Samples taken adjacent to the SS chambers were analyzed for Chloride (EPA Method 325.3) and TDS (EPA Method 160.1) at Eurofins Lancaster.

Statistical Analysis

All averages were reported with respective standard deviation (average +/- stdev). When comparing averages, propagation of error was used to calculate final standard deviation. Measurements demonstrating notable diurnal fluctuations were expressed in range as opposed to average in order to better encapsulate these trends. Statistical tests involving these measurements used either a maximum or minimum value.

Due to non-normality of data, uneven variance, and the presence of 0s, the non-parametric Kruskal Wallis test was used for comparison between groups, and a Dunn's post hoc test with Bonferroni correction was used when applicable. A beta regression was used to test significant relationships between proportion of survival and water quality predictor variables. The predictor variables used in the beta regression were either minimum or maximum values/concentrations for the respective parameter, in order to encapsulate the highest/lowest value/concentration organisms were exposed to. A p-value of ≤ 0.05 was used to determine whether or not relationships / comparisons between groups were deemed statistically significant, and p-values were rounded to 2 significant figures, when applicable. It should be noted that due to the use of non-parametric tests, significant differences reported are differences between groups, rather than mean values.

Samples analyzed for ammonia whose concentrations fell below the minimum detection limit (MDL) of 0.05 mg/L were replaced with 0 for the purpose of statistical analysis. In addition, faulty sonde data due to clogged or moved sensors were removed, as well as extreme outliers.

Results

In Situ Exposures

Travel control organisms yielded an average survival rate of 90.0% (± 7.1%), indicating transportation played a minimal role in organism mortality. Figure 5 shows *in situ* survival versus survival expressed as a percentage of travel controls.

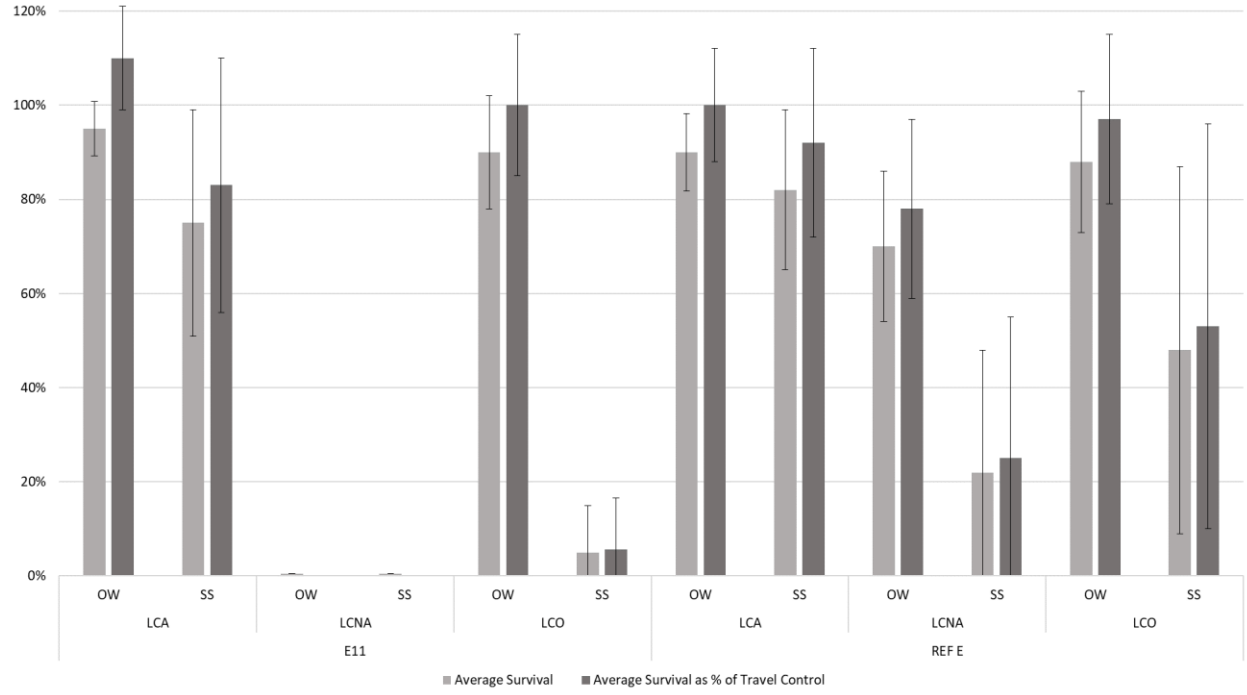

Figure 5: Average survival vs. Average survival expressed as a percentage of travel controls (90% ± 7.1%) for chambers and LC scenarios across both sites (E-11 and Ref-E). Error bars represent standard deviation.

Figure 6 summarizes average *H. azteca* survival for *in situ* exposures within OW and SS chambers and LC scenarios at sites Ref-E (Figure 6A) and E-11 (Figure 6B). Overall, survival at Ref-E (67% ± 32%) was higher than E-11 (44% ± 45%), however difference in survival across sites was not significant ($p = 0.18$).

Combined survival for overlying water (OW) and surficial sediment (SS) chambers showed aerated limnocorrals (LCA) at E-11 (85% ± 19%) and Ref-E (86 ± 13%) having the highest survival. Survival was lowest in non-aerated limnocorrals (LCNA) for both E-11 (0% ± 0%) and Ref-E (46% ± 32%). E-11 LCNA was the only treatment with complete mortality. LCNA was the sole LC scenario in which E-11 and Ref-E combined chamber survival differed (p=0.004). Survival in the treatment without a limnocorral (LCO) was higher in Ref-E (68% ± 35%) than E-11 (48% ± 47%), but the difference between groups was insignificant (p=0.48). LCNA and LCA survival differed at both E-11 ($p < 0.001$) and Ref-E ($p = 0.02$).

Mean survival in OW chambers was 31% (±40%) higher than SS chambers at Ref E and 35% (±60%) higher at E-11, but the difference between chambers was only significant at Ref-E (p=0.03). Ref-E OW (82% ± 15%) and SS survival (62% ± 46%) were greater than E-11 OW (62% ± 46%) and SS (27% ± 38%) survival, however, comparisons between OW (p=0.79) and SS (p=0.14) were not significant.

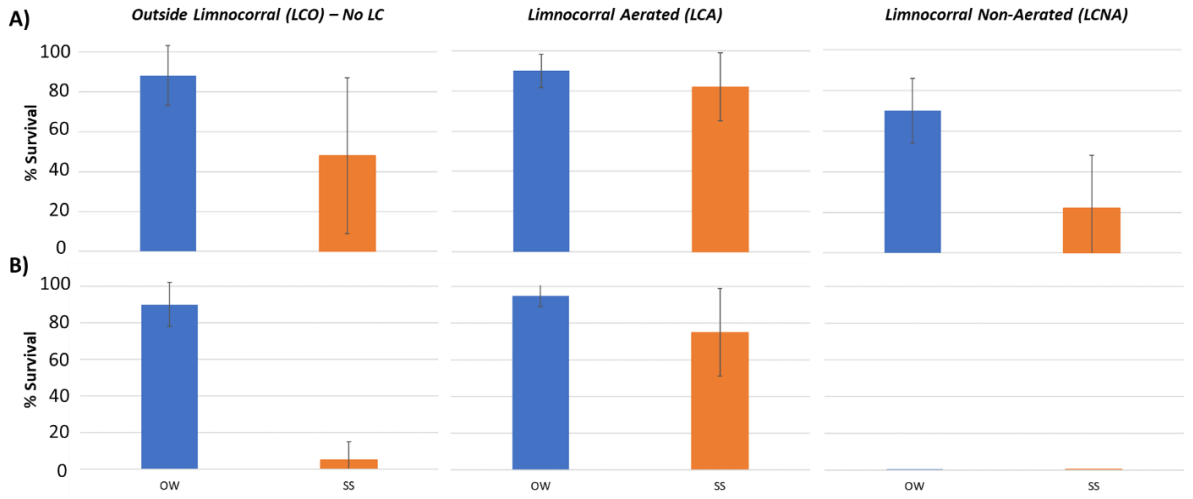

Figure 6: Average survival of *H. azteca* (%) for LC scenarios and chambers in Ref-E (A) and E-11 (B). Error bars represent standard deviation.

Dissolved Oxygen

Figure 7 depicts diurnal DO patterns over the duration of the exposure, including both OW and SS sensors within LC scenarios at Ref-E (Figure 7A) and E-11 (Figure 7B). The largest diurnal DO fluctuation was E-11 LCO; SS DO ranged from 1.4-20 mg/L, demonstrating lower minimum values than OW (2.3-19 mg/L). Both OW and SS DO in E-11 dropped below the minimum DO of 2.5 mg/L recommended for freshwater benthic organisms (US EPA, 2000b; Mattson et al., 2008). DO at Ref-E LCO exhibited a less dynamic diurnal cycle than Ref-E LCO, with SS ranging from 2.6-10.6 mg/L and OW 3.3-10.9 mg/L, staying above recommended minimum DO. LCA DO was relatively homogenous throughout the exposure, and DO ranges for E-11 (SS: 5.8-9.4, OW: 6.7-10.4 mg/L) and Ref-E (SS: 5.0-8.1, OW: 5.8-

7.6 mg/L) were most similar when comparing LC scenarios across sites. LCNA at E-11 was the only LC treatment across sites to have anoxic conditions (0 mg/L), which were observed on a nightly basis. Ref-E LCNA showed a diurnal DO pattern comparable to LCO but did not reach the same level of saturation (SS: 2.8-7.4, OW: 2.8-8.1 mg/L).

Tables 1 & 2 display daily WQ chamber water DO measured by a handheld DO meter. Comparison of chamber DO data to daytime DO data obtained by sondes (Figure 7) shows chamber DO consistently lower in concentration.

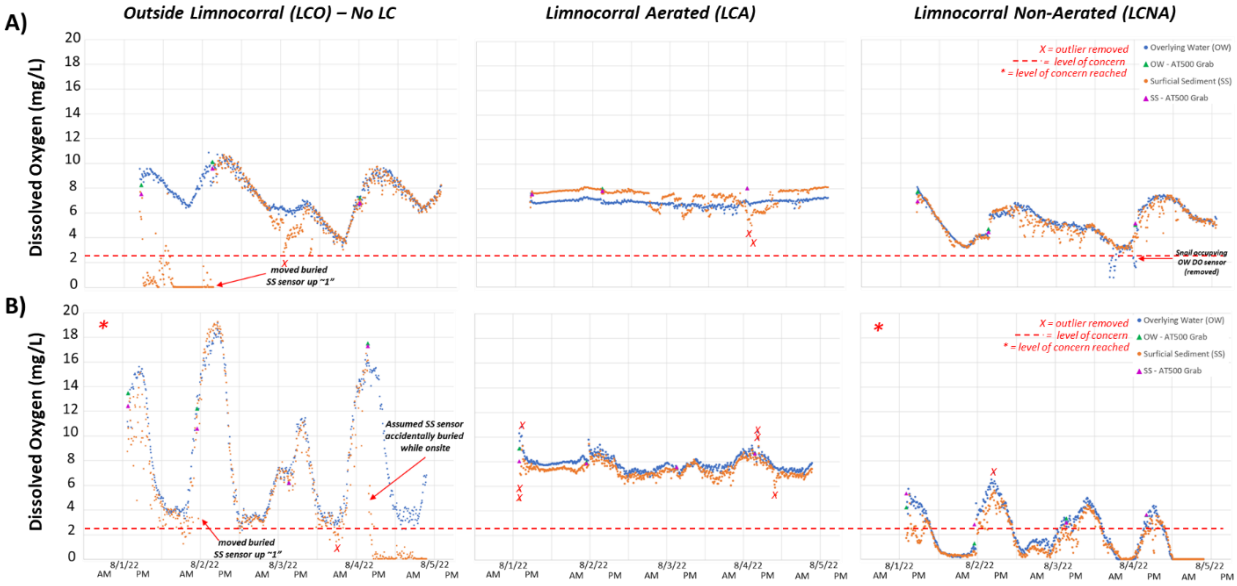

Figure 7: Sonde measurements of DO (mg/L) recorded across the duration of the exposure for SS and OW aligned sensors at Ref-E (A) and E-11 (B). Level of concern as specified by US EPA (US EPA, 2000b). Important to note only outliers interfering with maximum/minimum DO values were removed. AT500 were used for quality assurance.

Table 1: E-11 daily WQ chamber sample DO measurements.

Site	LC Scenario	Chamber	Day	Time	DO (mg/L)
E-11	LCNA	OW	1	11:20	2.73
			2	16:00	2.8
			3	16:30	3.8
			4	10:30	4.2
		SS	1	11:20	2.39
			2	16:00	2.6
			3	16:30	2.6
			4	10:30	3.3
	LCA	OW	1	11:35	6.63
			2	15:20	6.4
			3	15:40	7.1
			4	11:00	6.3
		SS	1	11:35	2.7
			2	15:20	3.2
			3	15:40	2.9
			4	11:00	3
	LCO	OW	1	11:30	4.3
			2	15:40	6.2
			3	16:00	9.6
			4	10:00	5.8
		SS	1	11:30	3.9
			2	15:40	4.8
			3	16:00	5.4
			4	10:00	3.5

Table 2: Ref-E daily WQ chamber sample DO measurements.

Site	LC Scenario	Chamber	Day	Time	DO (mg/L)
Ref-E	LCNA	OW	1	14:50	4.9
			3	12:45	3.6
			4	14:15	4.2
		SS	1	14:50	3.3
			3	12:45	2.8
			4	14:15	3.7
	LCA	OW	1	14:30	6.63
			3	12:20	6.03
			4	14:40	5.9
		SS	1	14:30	6.1
			3	12:20	5.6
			4	14:40	4.1
	LCO	OW	1	15:05	7.8
			3	12:30	6
			4	13:50	5.4
		SS	1	15:05	5.3
			3	12:30	3.1
			4	13:50	3.38

Ammonia

Sediment porewater airstone, SS, and OW chamber ammonia concentrations are summarized in Figure 8A (Ref-E) and Figure 8B (E-11). Combined OW and SS chamber ammonia across all LC scenarios were on average 0.33 mg/L (± 0.80) higher at E-11 (0.55 ± 0.61 mg/L) than Ref-E (0.22 ± 0.52 mg/L), and difference in chamber ammonia between E-11 and Ref-E were significant ($p = 0.002$). Ref-E (0.026 ± 0.032 mg/L). The E-11 (0.18 ± 0.15 mg/L) OW chambers differed in ammonia ($p = 0.02$), but this difference was not observed in SS chambers ($p = 0.06$), despite E-11 SS (0.92 ± 0.67 mg/L) demonstrating a higher average ammonia than Ref-E (0.41 ± 0.71 mg/L). Comparing chambers within the same site, E-11 OW and SS differed in concentration ($p = 0.009$), but this difference was not detected at Ref-E ($p = 0.08$).

Variations in chamber ammonia between LC scenarios was observed within E-11. The LCA (0.75 ± 0.55 mg/L) and LCO (0.080 ± 0.087 mg/L) differed ($p = 0.008$) as well as LCNA (0.82 ± 0.72 mg/L) and LCO ($p = 0.003$). Furthermore, E-11 LCNA SS chamber ammonia was the only chamber at both sites to show a consistent increase throughout the duration of the exposure (Figure 8B). Differences in ammonia amongst LC scenarios was not observed at Ref-E ($p = 0.20$). Comparing LC treatments across sites, LCA ($p = 0.002$) and LCNA ($p =$

0.002) differed between E-11 and Ref-E, with E-11 LCA and LCNA having higher ammonia than Ref-E. LCO was the only LC scenario that did not differ between sites ($p = 0.69$). Ammonia exceedances, with respect to the chronic (1.9 mg TAN/L) and acute (17 mg TAN/L) toxicity values established by US EPA's Ambient Water Quality for Ammonia (US EPA, 2013), were not observed at either site.

Sediment porewater ammonia had similar trends to chamber ammonia; E-11 (4.8 ± 2.4 mg/L) were on average 3.6 mg/L (±2.5) higher than Ref-E (1.1 ± 0.85 mg/L), and there was a difference between sites ($p < 0.001$). LC treatment sediment porewater ammonia was similar at both sites (E-11 ($p = 0.11$) or Ref-E ($p = 0.20$)). Similar to E-11 LCNA SS chambers, porewater concentrations steadily increased over the 4-day period. Porewater ammonia "exceedances" were not considered, as organisms were primarily exposed to overlying surface waters.

E-11 porewater ammonia was 4.6 mg/L (± 2.38) higher than OW chambers and 3.86 mg/L (± 2.46) higher than SS chambers. Ref-E porewater was 1.1 mg/L (± 0.85) higher than OW and 0.7 mg/L (± 1.1) higher than SS chambers. E-11 OW ($p < 0.001$), SS ($p < 0.001$), Ref-E OW ($p < 0.001$), and SS ($p = 0.02$) showed differences with surficial porewaters.

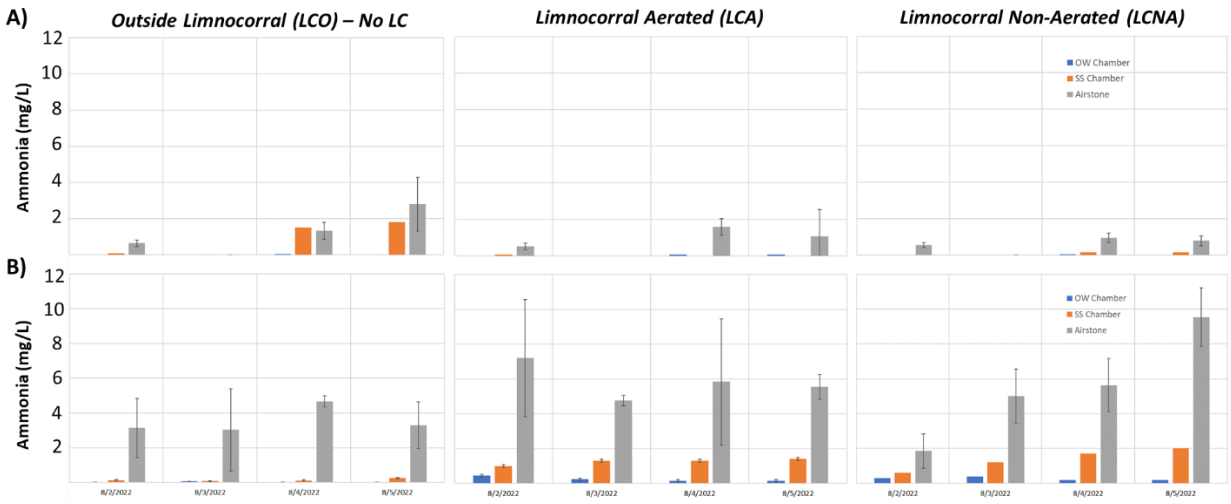

Figure 8: Ammonia (mg/L) for OW, SS, and sediment porewater airstone samples at Ref-E (A) and E-11 (B). Error bars represent standard deviation.

Additional WQ measurements

Diurnal temperature fluctuations (Figure 9), pH (Figure 10), and specific conductivity (Figure 11) over the duration of exposure by OW and SS aligned sensors. Temperature fluctuations were consistent across LC treatments within sites, and OW and SS sensors within LC scenarios demonstrated little to no variation. Overall range at E-11 (20.4- 28.4°C) was larger than Ref-E (23.5- 26.5°C). pH data revealed variations across OW and SS

positionings and LC scenarios; OW pH was higher than SS pH for E-11 LCA (OW: 8.1-8.7, SS: 7.8-8.3) and E-11 LCNA (OW: 7.7-8.6, SS: 7.5-8.4). Conversely, SS pH was higher for E-11 LCO (OW: 7.7-9.1, SS: 7.8-9.3), Ref-E LCO (OW: 7.7-8.9, SS: 8.0-9.1), and Ref-E LCA (OW: 7.8-8.3, SS: 8.0-8.5). Despite noticeable differences between chambers and LC scenarios, the overall pH range of E-11 (7.5-9.3) and Ref-E (7.2-9.1) were similar. E-11 LCO and Ref-E LCO both had pH values higher than the US EPA's limits established for freshwater (6.5-9.0) (US EPA, 1986); however, these high values were not sustained for extended periods of time. Specific conductivity exhibited contrasting patterns when comparing E-11 and Ref-E. Ref-E had a small fluctuation, ranging from 226-361 µS/cm, while E-11 was less consistent with higher values (218-585 µS/cm). OW and SS values at E-11 were similar apart from LCA, where SS values (438-586 µS/cm) were consistently higher than OW (352-468 µS/cm).

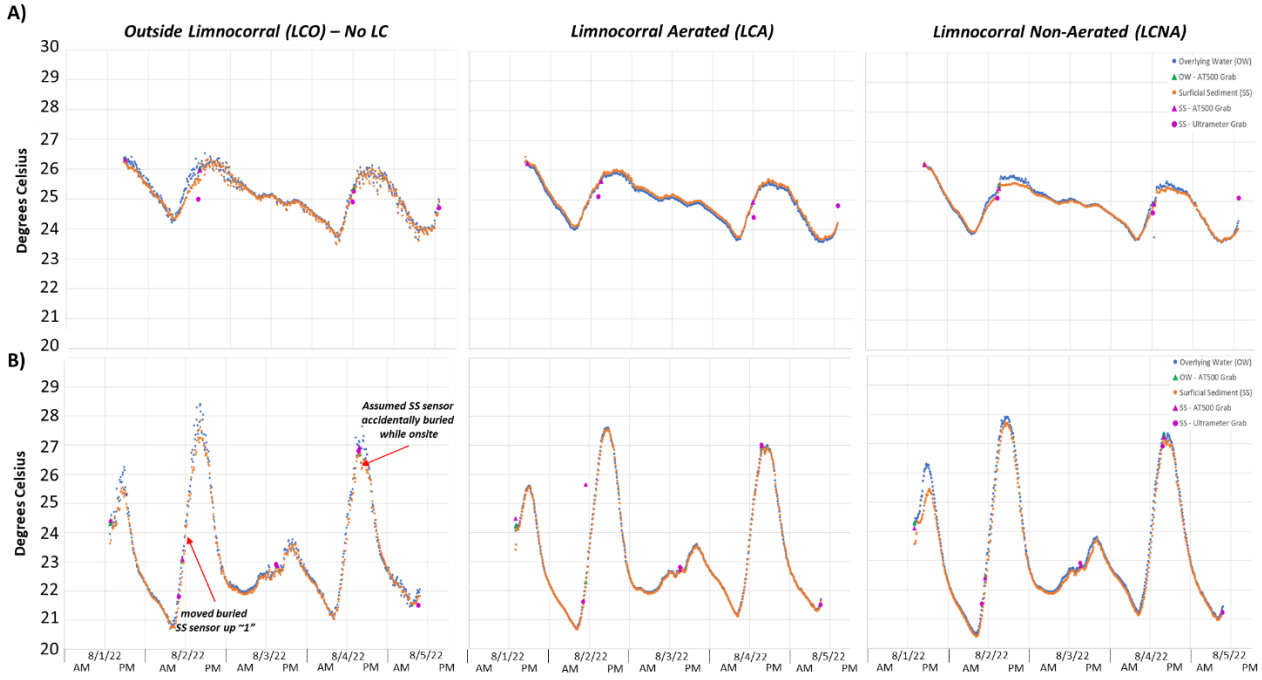

Figure 9: Sonde measurements of temperature (°C) across the duration of the exposure for OW and SS aligned sensors at Ref-E (A) and E-11 (B). AT500 were used for quality assurance.

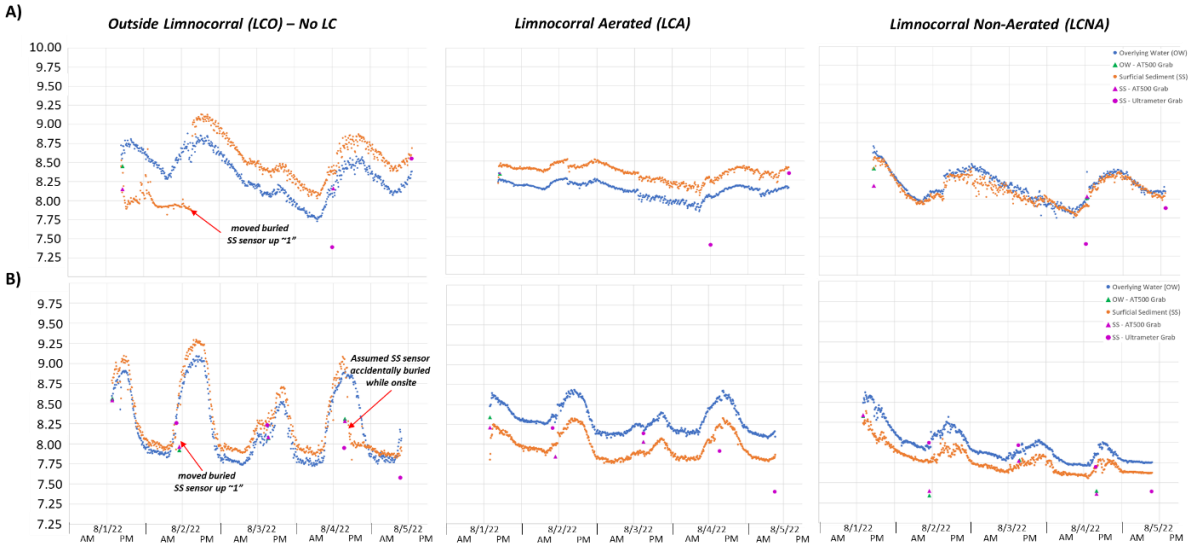

Figure 10: Sonde measurements of pH across the duration of the exposure for OW and SS aligned sensors at Ref-E (A) and E-11 (B). AT500 were used for quality assurance.

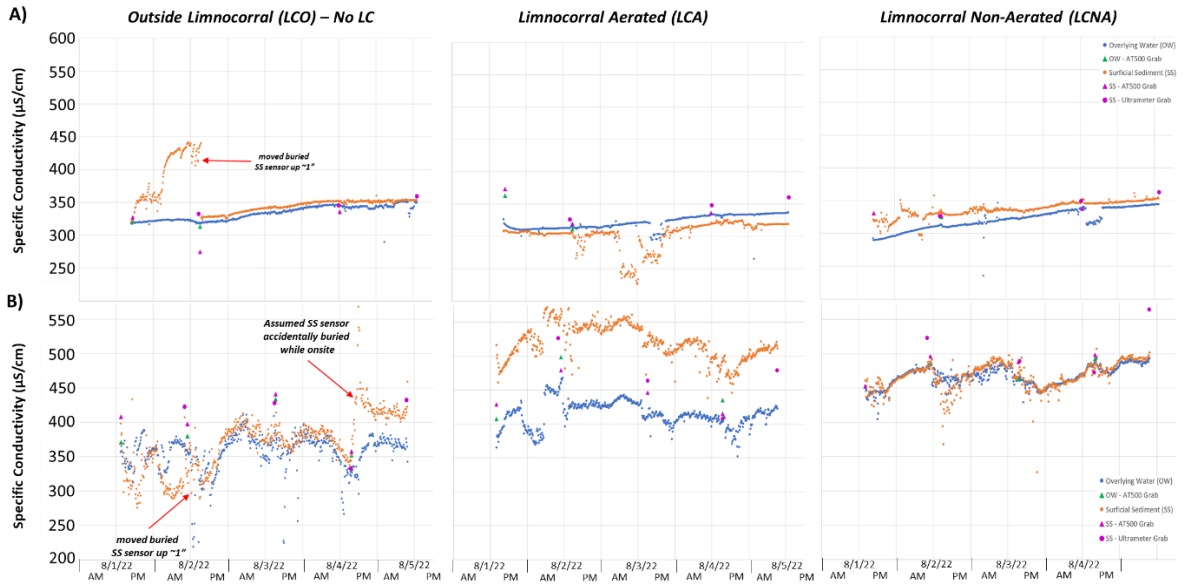

Figure 11: Sonde measurements of specific conductivity (µS/cm) across the duration of the exposure for OW and SS aligned sensors for Ref-E (A) and E-11 (B). AT500 were used for quality assurance.

Chloride and TDS sampled adjacent to SS chambers showed Ref-E chloride and TDS concentrations slightly lower than E-11, however chloride (p=0.08) and TDS (p=0.13) did

not differ. Chloride concentrations were below chronic (230 mg/L) and acute (860 mg/L) values established by US EPA Ambient Water Quality for Chloride (US EPA, 1988).

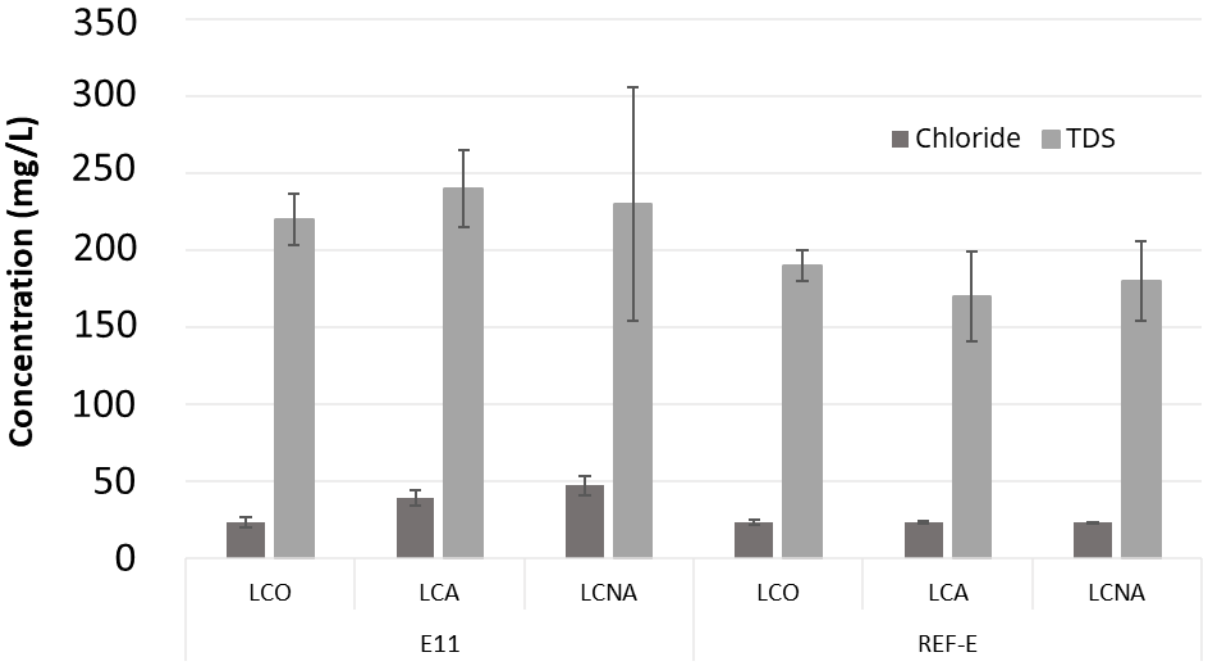

Figure 12: Chloride and TDS concentrations (mg/L) for samples adjacent to SS chambers at E-11 and Ref-E. Error bars represent standard deviation.

Water quality relationships to H. azteca survival

Water quality parameters intentionally left out of beta regression models included chlorides, TDS, temperature, and specific conductivity; as these did not exceed levels of concern and had no relationship to *H. azteca* survival. Sediment porewater airstone ammonia was also not included as these samples were not representative of the ammonia organisms were exposed to. There was a high correlation between maximum pH and maximum chamber ammonia at both E-11(0.79) and Ref-E (0.76), therefore pH was excluded to avoid issues with multicollinearity. The survival model for E-11 (R^2=0.64) showed a significant relationship between organism survival and minimum DO ($p < 0.001$). The relationship between survival and maximum chamber ammonia was not significant ($p = 0.28$). Both minimum DO ($p = 0.06$) and maximum ammonia ($p = 0.41$) were not significant predictors for organism survival in the Ref-E regression model ($R^2 = 0.21$).

Discussion

Diurnal dissolved oxygen fluctuations

Prior investigations of E-11 pointed towards diurnal DO cycles reaching stress-invoking levels for organisms residing within this site, which was corroborated by the results of this study. The DO threshold used in this study was 2.5 mg/L, which was established by US EPA's methods for measuring the toxicity and bioaccumulation of sediment-associated contaminants with freshwater invertebrates. This stress-inducing concentration was validated by a study done on *H. azteca* by Mattson et al. in 2008. The LC treatment representative of natural conditions (LCO) demonstrated pronounced fluctuations of DO at E-11, with near-bottom waters dropping below US EPA recommended guidelines at night. Reference site (Ref-E) LCO diurnal changes in DO; however, these fluctuations did not fall below levels of concern. It is important to note that evaluation of results was centered around sonde data in order to encapsulate DO across the entirety of the exposure, however, DO within organism chambers was observed to be consistently lower than respective sonde measurements due to restriction of flow within the chamber.

Minimum DO was the singular measured water quality parameter significantly associated with *H. azteca* survival at E-11, as seen from the results of the regression model. This relationship is further validated through comparison of reference site (Ref-E) and E-11 survival within aerated limnocorrals. When the DO stress was removed, LCA treatments showed Ref-E and E-11 DO to be similar and the only scenario in which survival was identical across sites. The greatest DO stress and mortality occurred at E-11 in LCNA chambers, where anoxic conditions were reached on a nightly basis.

Limited research has been conducted surrounding DO thresholds and sublethal impacts of hypoxic conditions on benthic macroinvertebrate in freshwater ecosystems (Mattson et al., 2007; Saari et al., 2018). These communities can be exposed to a wide range of DO levels, and the lack of data has raised concerns towards the validity of DO guidelines established for the protection of aquatic invertebrates (Saari et al., 2018, Irving at al., 2009). A study exposing *H. azteca* to varying DO concentrations over a 10-d period showed 100% juvenile mortality at concentrations ≤ 1.2mg/L, while no effects were observed at ≥ 2.9 mg/L (Irving et al., 2009). The thresholds recommended by Irving and et al. were refined by Mattson et al., who did an additional 10-d study with *H. azteca* and reported no effects at concentrations as low as 2.12 mg/L (Mattson et al., 2007). Both of these findings support the aforementioned relationships between organism survival and minimum DO concentrations observed in this investigation. It should be taken into consideration that not all invertebrate share the same range of DO tolerance; species belonging to the order Ephemeroptera, commonly used in bioassessments due to their abundance and sensitivity to pollution, have been shown to be less tolerant of low DO than *H. azteca*, with decreased survival at DO values up to 4.8 mg/L (Gaufin et al., 1974; Nebeker et al., 1972; Puckett et al., 2004). Previous line-of-evidence studies involving benthic macroinvertebrate assessments at E-11 showed it dominated by DO resistant gastropods, while Ephemeroptera were only ≥0.7% of the aquatic insect community, as compared to 4.7% and 6.0% at nearby undisturbed sites.

Numerous factors contribute to DO concentrations within a water column; increased photosynthetic rates during the daytime raises DO levels while processes such as respiration

and decomposition of organic matter lowers the oxygen in a system (Xu & Xu, 2016). Sediment oxygen demand (SOD) is often considered when investigating sources of oxygen depletion, with SOD referring to the rate at which biological and chemical processes consume oxygen at the sediment water interface (Coenen et al., 2019). Biological processes, otherwise known as biochemical oxygen demand (BOD), refer to the oxygen required by bacteria to break down organic matter (Hussain et al., 2021). Chemical oxygen demand (COD) encompasses oxygen depletion though oxidation processes occurring either within sediment or at the sediment interface (Rong et al., 2016). While no conclusions on the source of DO fluctuation can definitively be made from the current data, quantification of SOD could give valuable insight into the processes contributing to oxygen depletion within E-11.

Elevated ammonia concentrations

Ammonia at E-11 was notably higher than Ref-E, with emphasis on surficial sediment (SS) chambers and airstone samples; but did not have a significant relationship with organism survival. The results of the regression are verified when comparing site ammonia to *H. azteca* Species Mean Acute Value (SMAV, 192.6 mg/L) and Species Mean Chronic Value (SMCV, 29.17 mg/L), which are far above observed ammonia (US EPA, 2013). While ammonia was not high enough to induce toxicity with *H. azteca*, concentrations in E-11 LCA and LCNA SS chambers approached the US EPA chronic criterion magnitude (CCC) of 1.9 mg/L, especially when factoring in elevated pH and temperature (US EPA, 2013). The CCC value of 1.9 mg/L applies for 20℃ waters with a pH of 7.0, and this criterion decreases with raised temperature and pH due to increased invertebrate sensitivity (US EPA, 2013; Yan et al., 2019).

Although E-11 ammonia approached levels of concern within SS chambers at LCA and LCNA, these two treatments are not truly depicting natural conditions. Limnocorrals restrict the flow of water, and therefore prevent the dilution of contaminants (Alexander et al., 2016). Although limnocorrals were lowered once a day to allow for water to be exchanged, stagnant conditions and the confined nature of SS chambers likely reduced the effectiveness of this method for near-bottom waters. Evidence for this includes E-11 LCO chamber concentrations significantly differing from observed ammonia values for both respective limnocorral treatments (LCA and LCNA), while showing no difference when compared to chamber ammonia Ref-E. This suggests flow restriction has a role in elevated concentrations within E-11 LCA and LCNA, which organisms would not typically be exposed to. Ammonia in E-11 LCNA SS chambers increased throughout the exposure and E-11 LCNA was the only treatment to reach anoxic conditions. Anoxia can promote the release of ammonia from sediment due to decreased rates of ammonia assimilation (incorporation of ammonia into organic compounds) by microorganisms (Beutel, 2006). This trend is also supported by the daily increase in surficial sediment concentrations, which are representative of porewater ammonia.

Conversely, this effect was not observed at limnocorrals at Ref-E. A potential explanation for this is the significant difference between airstone ammonia concentrations at E-11 and Ref-E, with E-11 concentrations being on average 3.6 mg/L (±2.5) higher than Ref-E (Figure 8).

This ammonia gradient at E-11 suggests porewater could serve as a potential source for ammonia found in surface water samples (Carling et al., 2013, Frazier et al., 1996). Additional evidence for upwelling includes the increased range of specific conductivity observed at E-11, which is expected due to higher TDS being released in the upwellings against the sediment. The rate at which porewater ammonia leaches from sediment is influenced by many factors, including sediment type, seasonality, redox conditions, advection and disturbance (Xu et al., 2023; Frazier et al., 1996; Carling et al., 2013). Variability in these conditions resulting in higher/lower concentrations of surface water ammonia within sites where an ammonia gradient is present further emphasizes the importance of accounting for spatial and temporal heterogeneity with diversified sampling design.

Weight-of-evidence (WOE) approach evaluation

Assessment through utilization of several LOE in a WOE approach allowed for differentiation and quantification of stressors within this system that would have been difficult to achieve with only 1 or 2 LOE. However, WOE approaches are not without flaws; proper sampling design, accounting for extreme conditions, and consistent interpretation and decision making throughout the process are key to reducing uncertainty (Burton et al., 2002). An abundance of data is not useful if it is not of high quality, and inaccurate interpretations due to oversight of important trends can be an issue when dealing with large datasets. On the other hand, it is worth noting that the most obvious conclusion is not always the correct one, especially in the context of sites with COCs that approach or exceed water quality standards. Considering all lines of evidence and the different exposure pathways that could lead to the observed outcome is crucial; the presence of COCs can vary in terms of how large a role they have in ecological impairments, and attributing ecosystem degradation to the presence of a COC can lead to other important stressors being disregarded, thereby reducing the chance of successful site remediation and/or restoration.

The final LOEs evaluated in this multi-phased WOE approach allowed for differentiation between natural and anthropogenic stressors, with low survival of organisms at E-11 being ultimately attributed to diurnal DO fluctuation. Elevated ammonia levels within porewater demonstrated the potential for effluxion of ammonia from porewater into near-bottom waters, but these concentrations are likely diluted to levels below concern. However, as previously mentioned, a variety of factors are responsible for rates at which contaminants leach from porewater. Ammonia also has the potential to increase or decrease depending on seasonality and spatial drivers. Overall, this study highlights the complexity of addressing groundwater-surface water exposure in the face of multiple stressors, and how WOE approaches can help to establish stressor causality in these intricate environments. Future investigations could potentially include the quantification of sediment oxygen demand (SOD) to better understand the driving force behind pronounced diurnal DO fluctuations observed at E-11.

References

Alexander, A. C., Luiker, E., Finley, M., & Culp, J. M. (2016). Chapter 8—Mesocosm and Field Toxicity Testing in the Marine Context. In J. Blasco, P. M. Chapman, O. Campana, & M. Hampel (Eds.), *Marine Ecotoxicology* (pp. 239–256). Academic Press.

Altenburger, R., Brack, W., Burgess, R. M., Busch, W., Escher, B. I., Focks, A., Mark Hewitt, L., Jacobsen, B. N., de Alda, M. L., Ait-Aissa, S., Backhaus, T., Ginebreda, A., Hilscherová, K., Hollender, J., Hollert, H., Neale, P. A., Schulze, T., Schymanski, E. L., Teodorovic, I., Krauss, M. 2019. Future water quality monitoring: Improving the balance between exposure and toxicity assessments of real-world pollutant mixtures. *Environmental Sciences Europe*, 31(1), 12.

Bartlett, A., Struger, J., Grapentine , L. & Palace, V. 2016. Examining impacts of current-use pesticides in southern Ontario using in situ exposures of the amphipod Hyalella azteca. *Environmental Toxicology & Chemistry*, 35, 1224-1238.

Beutel, M. W. 2006. Inhibition of ammonia release from anoxic profundal sediments in lakes using hypolimnetic oxygenation. *Ecological Engineering*, 28(3), 271–279.

Blasco, C., & Picó, Y. 2009. Prospects for combining chemical and biological methods for integrated environmental assessment. *Trends in Analytical Chemistry,* 28(6), 745–757.

Burton GA, Johnston EL. 2010. Assessing contaminated sediments in the context of multiple stressors. *Environmental Toxicology and Chemistry,* 12, 2625-2643.

Burton, G. A., & Nordstrom, J. F. 2004a. An in situ toxicity identification evaluation method part I: Laboratory validation. *Environmental Toxicology and Chemistry*, 23(12), 2844–2850.

Burton, G. A., & Nordstrom, J. F. 2004b. An *In Situ* Toxicity Identification Evaluation Method Part II: Field Validation. *Environmental Toxicology and Chemistry.* 23(12), 2851–2855.

Burton, G. A., Cervi, E. C., Meyer, K., Steigmeyer, A., Verhamme, E., Daley, J., Hudson, M., Colvin, M., & Rosen, G. 2020. A Novel In Situ Toxicity Identification Evaluation (iTIE) System for Determining which Chemicals Drive Impairments at Contaminated Sites. *Environmental Toxicology and Chemistry*, 39(9), 1746–1754.

Burton, G. A., Cervi, E. C., Meyer, K., Steigmeyer, A., Verhamme, E., Daley, J., Hudson, M., Colvin, M., & Rosen, G. 2020. A Novel In Situ Toxicity Identification Evaluation (iTIE) System for Determining which Chemicals Drive Impairments at Contaminated Sites. *Environmental Toxicology and Chemistry*, 39(9), 1746–1754.

Burton, G. A., Chapman, P. M., & Smith, E. P. 2002. Weight-of-evidence approaches for assessing ecosystem impairment. *Human and Ecological Risk Assessment*, 8(7), 1657–1673.

Burton, G. A., Greenberg, M. S., Rowland, C. D., Irvine, C. A., Lavoie, D. R., Brooker, J. A., Moore, L., Raymer, D. F. N., & McWilliam, R. A. 2005. In situ exposures using caged

organisms: A multi-compartment approach to detect aquatic toxicity and bioaccumulation. *Environmental Pollution*, 134(1), 133–144.

Carling, G. T., Richards, D. C., Hoven, H., Miller, T., Fernandez, D. P., Rudd, A., Pazmino, E., & Johnson, W. P. 2013. Relationships of surface water, pore water, and sediment chemistry in wetlands adjacent to Great Salt Lake, Utah, and potential impacts on plant community health. *Science of The Total Environment*, 443, 798–811.

Chapman, P. M. 2007. Determining when contamination is pollution—Weight of evidence determinations for sediments and effluents. *Environment International,* 33(4), 492–501.

Chapman, P. M., Fairbrother, A., & Brown, D. 1998. A critical evaluation of safety (uncertainty) factors for ecological risk assessment. *Environmental Toxicology and Chemistry*, 17(1), 99–108.

Coenen, E. N., Christensen, V. G., Bartsch, L. A., Kreiling, R. M., & Richardson, W. B. 2019. Sediment Oxygen Demand: A Review of In Situ Methods. *Journal of Environmental Quality*, 48(2), 403–411.

Day, K. E., & Scott, I. M. 1990. Use of acetylcholinesterase activity to detect sublethal toxicity in stream invertebrates exposed to low concentrations of organophosphate insecticides. *Aquatic Toxicology*, 18(2), 101–113.

Dias, N. C., & Poole, C. F. 2002. Mechanistic study of the sorption properties of OASIS® HLB and its use in solid-phase extraction. *Chromatographia*, 56(5–6), 269–275.

Dias, N. C., & Poole, C. F. 2002. Mechanistic study of the sorption properties of OASIS® HLB and its use in solid-phase extraction. *Chromatographia*, 56(5–6), 269–275.

Ellman GL, Courtney KD, Andres V, Featherstone RM. 1961. A new and rapid colorimetric determination of acetylcholinesterase activity. *Biochemistry Pharmacology,* 7, 88–95.

Fanelli RM, Cashman MJ, Porter AJ. 2022. Identifying Key Stressors Driving Biological Impairment in Freshwater Streams in the Chesapeake Bay Watershed, USA. *Environmental Management, 70*(6), 926–949.

Fierro, P., Bertrán, C., Tapia, J., Hauenstein, E., Peña-Cortés, F., Vergara, C., Cerna, C., & Vargas-Chacoff, L. 2017. Effects of local land-use on riparian vegetation, water quality, and the functional organization of macroinvertebrate assemblages. *Science of The Total Environment*, 609, 724–734.

Frazier, B. E., Naimo, T. J., & Sandheinrich, M. B. 1996. Temporal and vertical distribution of total ammonia nitrogen and un-ionized ammonia nitrogen in sediment pore water from the upper Mississippi River. *Environmental Toxicology and Chemistry*, 15(2), 92–99.

Ganie, S. Y., Javaid, D., Hajam, Y. A., & Reshi, Mohd. S. 2022. Mechanisms and treatment strategies of organophosphate pesticide induced neurotoxicity in humans: A critical appraisal. *Toxicology*, 472, 153-181.

Gaufin, A. R., Clubb, R., & Newell, R. 1974. Studies on the Tolerance of Aquatic Insects to Low Oxygen Concentrations. *The Great Basin Naturalist*, 34(1), 45–59.

Govenor, H., Krometis, L. A. H., & Hession, W. C. 2017. Invertebrate-Based Water Quality Impairments and Associated Stressors Identified through the US Clean Water Act. *Environmental Management*, 60(4), 598–614.

Hayman, N. T., Rosen, G., Colvin, M. A., Chadwick, B. D., Rao, B., Athanasiou, D., Rakowska, M., Drygiannaki, I., Burton Jr, G. A., & Reible, D. D. 2020. Seasonal Toxicity Observed with Amphipods (Eohaustorius estuarius) at Paleta Creek, San Diego Bay, USA. *Environmental Toxicology and Chemistry*, 39(1), 229–239.

Ho, K. T., Gielazyn, M. L., Pelletier, Marguerite. C., Burgess, Robert. M., Cantwell, M. C., Perron, M. M., Serbst, J. R., & Johnson, R. L. 2009. Do Toxicity Identification and Evaluation Laboratory-Based Methods Reflect Causes of Field Impairment? *Environmental Science & Technology,* 43(17), 6857–6863.

Hussain, F., Yu, H.W., Chon, K., Lee, Y.G., Eom, H., Chae, K.J., & Oh, S.E. 2021. Real-time biomonitoring of oxygen uptake rate and biochemical oxygen demand using a novel optical biogas respirometric system. *Journal of Environmental Management*, 277, 111467.

Irving, E. C., Liber, K., & Culp, J. M. 2004. Lethal and sublethal effects of low dissolved oxygen condition on two aquatic invertebrates, *Chironomus tentans* and *Hyalella azteca*. *Environmental Toxicology and Chemistry*, 23(6), 1561-1566.

Julien R., Adamkiewicz G. & Levy J. et al. 2008. Pesticide loadings of select organophosphate and pyrethroid pesticides in urban public housing. *Journal of Exposure Science and Environmental Epidemiology*, 18, 167–174.

Laetz, C. A., Baldwin, D. H., & Scholz, N. L. 2020. Sublethal neurotoxicity of organophosphate insecticides to juvenile coho salmon. *Aquatic Toxicology*, 221, 105424.

Luo, Y.S., Chen, Z., Hsieh, N.H., & Lin, T.E. 2022. Chemical and biological assessments of environmental mixtures: A review of current trends, advances, and future perspectives. *Journal of Hazardous Materials,* 432, 128658.

Madrid, Y., & Zayas, Z. P. 2007. Water sampling: Traditional methods and new approaches in water sampling strategy. *Trends in Analytical Chemistry*, 26(4), 293–299.

Maggio, S. A., & Jenkins, J. J. 2022. Multi- and Trans-Generational Effects on Daphnia Magna of Chlorpyrifos Exposures. *Environmental Toxicology and Chemistry,* 41(4), 1054–1065.

Mattson, V. R., Russell Hockett, J., Highland, T. L., Ankley, G. T., & Mount, D. R. 2008. Effects of low dissolved oxygen on organisms used in freshwater sediment toxicity tests. *Chemosphere*, 70(10), 1840–1844.

Michalaki, A., McGivern, A. R., Poschet, G., Büttner, M., Altenburger, R., & Grintzalis, K. 2022. The Effects of Single and Combined Stressors on Daphnids—Enzyme Markers of Physiology and Metabolomics Validate the Impact of Pollution. *Toxics*, 10(10).

Moore, M. T., Huggett, D. B., Gillespie, W. B., Rodgers, J. H., & Cooper, C. M. 1998. Comparative Toxicity of Chlordane, Chlorpyrifos, and Aldicarb to Four Aquatic Testing Organisms. *Arch. Environ. Contam. Toxicol.*, 34, 152–157.

Naddy, R. B., Johnson, K. A., & Klaine, S. J. (2000). Response of Daphnia magna to pulsed exposures of chlorpyrifos. Environmental Toxicology and Chemistry, 19(2), 423–431.

Nebeker, A. V. 1972. Effect of Low Oxygen Concentration on Survival and Emergence of Aquatic Insects. *Transactions of the American Fisheries Society*, 101(4), 675–679.

Palmer, M. A., Menninger, H. L., & Bernhardt, E. 2010. River restoration, habitat heterogeneity and biodiversity: A failure of theory or practice? *Freshwater Biology*, 55, 205–222.

Phipps, G. L., Mattson, V. R., & Ankley, G. T. 1995. Environmental Contamination a n d Toxicology Relative Sensitivity of Three Freshwater Benthic Macroinvertebrates to Ten Contaminants. *Arch. Environ. Contam. Toxicol.*, 28, 281–286.

Plomp, R. D., Klemish, J. L., & Pyle, G. G. 2020. The Single and Combined Effects of Wildfire Runoff and Sediment-Bound Copper on the Freshwater Amphipod Hyalella azteca. *Environmental Toxicology and Chemistry*, 39(10), 1988–1997.

Puckett, R. T., & Cook, J. L. 2004. Physiological tolerance ranges of larval Caenis latipennis (Ephemeroptera: Caenidae) in response to fluctuations in dissolved oxygen concentration, pH and temperature. *The Texas Journal of Science*, 56(2), 123–131.

Rasmussen, J. J., Wiberg-Larsen, P., Kristensen, E. A., Cedergreen, N., & Friberg, N. (2013). Pyrethroid effects on freshwater invertebrates: A meta-analysis of pulse exposures. *Environmental Pollution*, 182, 479–485

Rong, N., Shan, B., & Wang, C. 2016. Determination of Sediment Oxygen Demand in the Ziya River Watershed, China: Based on Laboratory Core Incubation and Microelectrode Measurements. *International Journal of Environmental Research and Public Health*, 13(2), 232.

Rosen, G., Chadwick, B., Poucher, S. Greenberg, M., Burton, G. 2009. In Situ Estuarine and Marine Toxicity Testing- A Review, Including Recommendations for Future Use in Ecological Risk Assessment. Technical Report. SSC Pacific, San Diego, CA.

Saari, G. N., Wang, Z., & Brooks, B. W. 2018. Revisiting inland hypoxia: Diverse exceedances of dissolved oxygen thresholds for freshwater aquatic life. *Environmental Science and Pollution Research*, 25(4), 3139–3150.

Schulz R. (2004). Field studies on exposure, effects, and risk mitigation of aquatic nonpoint-source insecticide pollution: A review. *Journal of Environmental Quality*, 33, 419–448.

Sojka, M., & Jaskuła, J. (2022). Heavy Metals in River Sediments: Contamination, Toxicity, and Source Identification—A Case Study from Poland. *International Journal of Environmental Research and Public Health*, 19(17), Article 17.

Steigmeyer, A. J., Zhang, J., Daley, J. M., Zhang, X., & Burton, G. A. 2017. An *in situ* toxicity identification and evaluation water analysis system: Laboratory validation. *Environmental Toxicology and Chemistry*, 36(6), 1636–1643.

Suter, G. W., Norton, S. B., & Cormier, S. M. 2002. A methodology for inferring the causes of observed impairments in aquatic ecosystems. *Environmental Toxicology and Chemistry*, 21(6), 1101–1111.

US EPA. 1986. Quality Criteria for Water. United States Environmental Protection Agency Office of Water Regulations and Standards, Washington, DC. EPA 440/5-86-001.

US EPA. 1988. Ambient Water Quality Criteria for Chloride. EPA 440/5-88-001. Office of Water Regulations and Standards, Washington, DC.

US EPA. 2000a. Stressor Identification Guidance Document. EPA 822B-00-025. Office of Water and Office of Research and Development, Washington, DC.

US EPA. 2000b. Methods for measuring the toxicity and bioaccumulation of sediment-associated contaminants with freshwater invertebrates, second ed. EPA/600/R-99/064. US Environmental Protection Agency, Washington, DC.

US EPA. 2002. Short-term Methods for Estimating the Chronic Toxicity of Effluents and Receiving Waters to Marine and Estuarine Organisms. EPA-821-R-02-014. Office of Water, Washington, DC.

US EPA. 2007. Sediment Toxicity Identification Evaluation (TIE) Phases I, II, and III Guidance Document. EPA/600/R-07/080. Office of Research and Development, Washington, DC.

US EPA. 2011. A Primer on Using Biological Assessments to Support Water Quality Management. EPA 810-R-11-01. Office of Science and Technology and Office of Water, Washington, DC.

US EPA. 2013. Aquatic Life Ambient Water Quality Criteria for Ammonia- Freshwater. EPA 822-R-18-002. Office of Water, Washington DC.

Wolff, B. A., Pomeranz, J. P. F., Kotalik, C. J., Hall, E. K., & Clements, W. H. 2022. Habitat restoration for brown trout (Salmo trutta) has limited effects on macroinvertebrate communities in a historically metal-contaminated stream. *Integrated Environmental Assessment and Management,* 18(4), 1047–1055.

Xu, S., Lu, J., Chen, L., Luo, W., & Zhu, S. 2023. Experiment on Sediment Ammonia Nitrogen Release of Chaohu Lake in Varying Hydrodynamic Disturbance. *Sustainability*, 15(2), 1581.

Xu, Z., & Xu, Y. J. 2016. A Deterministic Model for Predicting Hourly Dissolved Oxygen Change: Development and Application to a Shallow Eutrophic Lake. *Water*, 8(2), Article 2.

Yan, Z.G., Fan, J.T., Zheng, X., Wang, S.P., Guo, X.S., Zhang, T.X., Yang, S.W., & Zhang, Y.Z. 2019. Neglect of Temperature and pH Impact Leads to Underestimation of Seasonal Ecological Risk of Ammonia in Chinese Surface Freshwaters. *Journal of Chemistry*.

Appendix A: iTIE Stanard Operating Procedure (SOP)

Trident Deployment

1. Gather the equipment and materials described in the equipment list (should all be located in iTIE toolbox and bazooka case)
2. Clean the water sampling probes, screens and tips with warm water and a lab grade detergent such as Alconox or Liquinox, using a soft bristle brush. Rinse thoroughly with DI water and allow to dry.
3. Assemble the probes onto the hex-head (and extension plates if needed) in the desired configuration.
4. Install the stopper plate including the stopper plate pole and adjustment rod, adjusting stopped plate to desired depth.
5. Add metal mesh screens over each one of the probes
6. Install second metal filter over metal screens
7. Fill gap between the probe and second metal filter with glass beads
    a. Done by putting glass beads into a cap and adding DI water, then carefully pouring into the filter and spraying with DI to ensure evenly distributed
        i. Make sure not to overfill, as cap will be added on top.
8. Once full (not too full), add caps on the top of each probe
9. Connect ¼" tubing to adapter located above the stopper plate
    a. Use ¼" tube cutter to cut tube
        i. Ensure tube is long enough to reach the depth of deployment for the probe and still connect to adapter within cooler unit.
    b. Use ¼" grooving tool to groove both ends of the tube
        i. Done by pulling the blade out, pushing the tube in, and pushing the tube all of the way in and rotating counterclockwise (if looking towards the end in which the tube is inserted)
    c. Connect tube to adapter by loosening the adapter, inserting the tube, tightening slightly, pulling the tube out so that it lodges in the groove, and tightening the rest of the way
10. Connect the other end of the tube to the adapter within the iTIE cooler unit
    a. Thread tube through black connector located on the side of the cooler
    b. Adapter works same way as adapter on Trident probe, make sure tube is grooved
    c. After the tube is inserted into the adapter, tighten black connector

Priming Oxygen System

1. Oxygen system will be primed with porewater
2. Turn on the oxygen supply by rotating the circular valve on oxygen canister (located behind box containing sample bottles) counterclockwise
    a. When on, should read 45-50 PSI
3. Turn gray valve on regulator parallel to allow oxygen flow

   a. To vent (must be done when shutting off oxygen) rotate gray valve next to oxygen tubing so that it is parallel to tube
4. Turn 3-way T valve so that T is upside down
5. Attach auxiliary tube to tubing connected to peristaltic pump
   a. Figure 26 shows where auxiliary tube is connected
   b. Have end of tube coming out of peristaltic pump flowing into beaker
6. Turn on peristaltic pump and have run on battery with the speed at 0 initially
   a. Choose which way you want the pump to run with switch located about text reading “Drive Controls”
   b. Flip switch from off to “run” and turn the speed up
7. Run peristaltic pump until number of bubbles is significantly reduced
   a. Can turn system on side (so that oxygen coil is lying vertically instead of horizontally) to help get rid of the bubbles
   b. Can also test DO content to ensure oxygen system working

Attaching and priming versa pump tubing

1. Thread Versa pump tubing through the side of the cooler
2. Connect tubes labeled “IN” to adapters on iTIE units, connect tubes labeled “OUT” to sample bottles
   a. Tubes are color coded to match color on Mobius app- black sharpie indicates “out”
   b. Tubing from pump 1 should attach to iTIE unit and sample bottle on far lefthand side, increasing in number as you move to the right
      i. Ensure the “IN” and “OUT” tubes attached to iTIE unit and corresponding sample bottle are from the same pump
   c. Connecting tubes to iTIE units (“IN” tubes):
      i. Loosen white grooved piece
      ii. Insert tube into adapter and slightly tighten grooved piece
      iii. Pull on the tube (as if trying to pull it out) and it should stick in the groove, tighten rest of way
   d. Connecting tubes to sample bottles (“OUT” tubes):
      i. Push pump tube into white tubing coming out from the top of the sample bottle
3. Put auxiliary tube in source of culture control water (IEW)
4. Turn T valve so that T is right side up
5. Use instant dose to dose each chamber
6. Empty sample bottles and iTIE units of water once primed
   a. To empty iTIE units:
      i. Remove top adapter from unit, hold finger on top port to keep pressure
      ii. Remove bottom adapter from unit, keeping finger on top port to prevent water from escaping
      iii. Once bottom adapter is removed, put finger on bottom port to prevent water escape

iv. Remove top cap and pour out water
v. Reattach units

Adding Resins

1. Remove top half of iTIE unit so the resin chamber is open
2. Add in layer of glass wool
3. Prewet resins with IEW so they are damp
4. Add in resin, wetting it with IEW once it is in the chamber
5. Once all 5 grams of the resin are added, extract any extra water using falcon pipette
6. Add in layer of glass wool on top of resin
7. Reattach units

Adding Organisms

1. Remove tops of iTIE units
2. Manually pour in culture water
3. Add in organisms (10 per unit) along with organism food
4. Replace top caps
    a. ***When replacing top caps hold onto bottom of unit- pressure can cause bottom to pop off***

Initiating Run

1. Reset the daily dose on the Mobius app for each pump to avoid issues with going over the maximum daily dose (daily dose will be higher than 0 due to priming)
    a. Open settings (within the Mobius app, not the tablet settings) and change the date (can change it to whatever desired date, does not necessarily matter)
        i. The main concern is TIME- make sure the time is set to the proper time needed for the scheduled runs to start
    b. After resetting date, all pumps should show 0 mL for daily dispensed volume
2. Turn T valve so that bottom of T is facing away from tubing
3. Make sure oxygen is on and functional
4. Use schedule feature to schedule a run for the desired time / flow rate (12 hours, 20 mL / hour, 0.33 mL/min)
    a. First confirm time and date in Mobius app- this is not synced to time and date of the tablet and could cause issues with a scheduled run
    b. Click on pump and click “dosing schedule”
        i. If the mode is “continuous”, change to custom
    c. Click the blue plus sign in the bottom left corner to add a scheduled run.
    d. Once button is clicked, tap on any time along the left hand side to add the run. The screen below should appear after a time is clicked- adjust the time using the “from” and “to” sections. Adjust dose by clicking on “dosage”.

    e. Once returned to home screen of the selected pump, if there is a “play” button to the right of the eyedropper, the schedule will not run for that pump. Press the play to tell the pump to run on the schedule- should turn into “stop” button once this is done.
    f. Runs scheduled for 24 hours will restart after the 24-hour period
5. Make sure blue light is pulsing for each pump and that the pumps are moving (can be hard to tell, blue light is best indicator)
6. Once run is over, press the “stop” button on the main screen of each pump

Breakdown

Trident

1. Dunk in water a few times to remove excess sediment
2. Take the metal filter and screens off the trident probes and remove the glass beads
    a. Rinse probes and metal screens with hose
3. After Trident is removed, remove the pore water tubing from the cooler

Cooler

1. Turn OFF oxygen system
2. Remove iTIE units using steps described above (removing top adapter, finger to keep pressure, etc)
3. Put mysids into travel containers
4. Replace iTIE units
5. Remove versa pump tubing

Equipment List

- Trident
    - 1 push pole
    - Slide hammer
- Tool box
    - Glass beads
    - Trident accessories (metal coverings, caps)
    - Tubing (black wheel, medium diameter)
    - Tubing (brown wheel, small diameter)
    - Tube cutters
    - Extra oxygen tank
    - Tube grooving tool
- Versa pump box
- Tablet
- Cooler

- Peristaltic pump
    - Peristaltic pump tubing
- Container of DI water
    - Spray bottle for DI water
- Carboy of IEW
- Organisms
    - Travel and lab controls
- Beakers
- Extra sample bottles
- DO meter
- pH meter
- Thermometer
- Liquinox soap -> spray bottle
- Resins (5G each, but bring extra)
    - Zeolite
    - Chelex
    - GAC
    - Glass Wool
- Falcon pipettes
- Organism counting trays
- Containers for transporting organisms back

Appendix B: iTIE Deployment Data

Table S1: Dissolved oxygen testing – oxygen system kept off

Dissolved Oxygen (mg/L)	
Source	*Oxygen Off*
0.7	2.5
0.7	2.6
0.7	2.7
0.6	3.9
0.6	3.6
0.6	2.79
0.78	3.5

Table S2: Dissolved oxygen testing – oxygen system turned on

Dissolved Oxygen (mg/L)	
Source	*Oxygen On*
0.38	5.85
0.28	7.7
0.67	10.75
0.67	9.94
0.5	10.05
0.5	9.3
0.78	6.12
1.12	10

Table S3: Dissolved oxygen testing (Figure 1)

	Avg DO (mg/L)	**S.D.**
Source	0.638667	0.193349
O2 OFF	3.084286	0.564856
O2 ON	8.71375	1.904505

Table S4: *A. bahia* survival (Figure 6)

Resin	Survival (n=10)
HLB	4
Chelex	8
Glass Wool	4
GAC	0
Lab Control	10

Table S5: Paleta Creek post-exposure WQ (Survival for all units = 0)

iTIE Unit	Resin	DO (mg/L)	Temp °C	Salinity (ppt)
1	Glass Wool	6.78	21.6	33.7
2	GAC	2.6	22	33.9
3	Chelex	6.02	21.9	33.9
4	HLB	8	21.5	33.9

Table S6: Fleming Creek post-exposure WQ (Figure 8)

Temperature for all units = 14°C

iTIE Unit	Resin	D. magna Survival (n=10)	H azteca Survival (n=10)	DO (mg/L)	Sample Bottle Volume (mL)
1	Glass Wool	8	9	9.87	35
2	Chelex	7	9	9.88	53
3	GAC	9	10	9.7	98
4	Zeolite	10	8	9.55	214

Appendix C: AChE Data and Statistical Analysis

Raw data from plate readings available upon request.

Table S7: HLB 24-hr exposure *H. azteca* survival and WQ data

iTIE Unit	Resin	Survival (n=10)	DO (mg/L)	Temp ℃	pH	Sample Bottle Volume (mL)
Source	N/A	N/A	7.32	18.8	7.9	N/A
1	HLB	10	6.87	19.7	7.68	640
2	HLB	10	7	19.3	7.63	660
3	HLB	10	6.87	19.4	7.68	620
4	Glass Wool	10	7.08	19	7.69	660
5	Glass Wool	10	6.92	19.1	7.76	660
6	Glass Wool	9	7.32	18.8	7.91	650

Table S8: C18 24-hr *H. azteca* exposure survival and WQ data

iTIE Unit	Resin	Survival (n=10)	DO (mg/L)	Temp ℃	pH	Sample Bottle Volume (mL)
Source	N/A	N/A	7.28	19	7.82	N/A
1	C18	10	7.18	20.6	7.42	650
2	C18	10	6.94	20	7.51	680
3	C18	10	7.14	19.9	7.59	680
4	Glass Wool	10	6.9	19.9	7.51	670
5	Glass Wool	8	6.85	19.8	7.56	630
6	Glass Wool	10	6.67	19.8	7.71	630

Table S9: Amberlyst-15 24-hr *H. azteca* exposure survival and WQ data

iTIE Unit	Resin	Survival (n=10)	DO (mg/L)	Temp ℃	pH
Source	N/A	N/A	6.84	18.9	7.89
1	Amberlyst-15	0	6.25	19.3	2.27
2	Amberlyst-15	0	6.34	19	2.32
3	Amberlyst-15	0	6.35	19	2.3
4	Glass Wool	10	6.76	18.9	7.6
5	Glass Wool	10	6.77	19.1	7.64
6	Glass Wool	10	6.76	19	7.66

Table S10: GAC *H. azteca* survival and DO data (Figure 13)

iTIE Unit	Resin	Survival (n=10)	DO (mg/L)
1	GAC	10	4.5
2	GAC	0.01	2.5
3	GAC	0.01	2.8
4	Glass Wool	10	7.02

Table S11: Specific activity data and calculations

		Replicate A			Replicate B			Replicate C							Mean enzyme activity
Vial ID #	Assay Vol	ABS1	ABS2	delta ABS/min	ABS1	ABS2	delta ABS/min	ABS1	ABS2	delta ABS/min	Avg delta ABS	SD	CV	[Protein]	per gram of protein
	(mL)	(2 min)	(4 min)		(2 min)	(4 min)		(2 min)	(4 min)					(mg/mL)	(umol min-1 g-1)
HLB															
2-12-2023_GW4S1	0.30	1.0910	1.2750	0.0920	1.0450	1.2310	0.0930	1.1380	1.2570	0.0595	0.0925	0.0005	0.5405	0.8567	68.0525
2-12-2023_GW4S2	0.30	1.0500	1.2100	0.0800	1.0520	1.2170	0.0825	1.0900	1.2170	0.0635	0.0753	0.0084	11.1895	0.8894	53.3805
2-12-2023_GW5S2	0.30	1.0940	1.2210	0.0635	N/A	N/A	N/A	1.0120	1.1790	0.0835	0.0735	0.0100	13.6054	0.6475	71.5421
2-12-2023_GW6S1	0.30	0.8810	1.0140	0.0665	0.8970	0.9920	0.0475	0.9480	1.0340	0.0430	0.0453	0.0022	4.9724	0.4903	58.1689
2-12-2023_GW6S2	0.30	0.9620	1.0970	0.0675	0.9410	1.1040	0.0815	0.9510	1.0940	0.0715	0.0735	0.0059	8.0107	0.4861	95.2941
2-12-2023_HLB1S1	0.30	1.0610	1.3000	0.1195	1.1440	1.3510	0.1035	1.0660	1.2980	0.1160	0.1130	0.0069	6.0777	0.7694	92.5583
2-12-2023_HLB1S2	0.30	1.1230	1.2790	0.0780	1.1040	1.2480	0.0720	1.0280	1.1660	0.0690	0.0730	0.0037	5.1256	0.6713	68.5414
2-12-2023_HLB2S1	0.30	1.0940	1.2370	0.0715	0.9970	1.1460	0.0745	0.9760	1.1290	0.0765	0.0742	0.0021	2.7705	0.5972	78.2685
2-12-2023_HLB2S2	0.30	1.0190	1.1600	0.0705	1.0350	1.1560	0.0605	0.9810	1.1210	0.0700	0.0670	0.0046	6.8668	0.4906	86.0797
2-12-2023_HLB3S1	0.30	1.0090	1.1950	0.0930	0.9960	1.1890	0.0965	1.0170	1.1980	0.0905	0.0933	0.0025	2.6366	0.6258	93.9923
2-12-2023_HLB3S2	0.30	0.9530	1.1490	0.0980	1.0300	1.1880	0.0790	N/A	N/A	N/A	0.0885	0.0095	10.7345	0.5981	93.2644
C18															
2-15-2023_C181S1	0.30	1.5140	1.8330	0.1595	1.4520	1.7460	0.1470	1.4480	1.7610	0.1565	0.1543	0.0053	3.4523	0.8885	109.4802
2-15-2023_C181S2	0.30	1.2340	1.4580	0.1120	1.1800	1.4090	0.1145	1.2460	1.4500	0.1020	0.1095	0.0054	4.9321	0.9428	73.2013
2-15-2023_C182S1	0.30	1.1980	1.3910	0.0965	1.0750	1.2390	0.0820	1.2070	1.3570	0.0750	0.0845	0.0090	10.5960	0.7727	68.9230
2-15-2023_C182S2	0.30	1.1690	1.3370	0.0840	1.1080	1.2930	0.0925	1.1650	1.3320	0.0835	0.0867	0.0041	4.7652	0.8189	66.7024
2-15-2023_C183S1	0.30	1.2160	1.4720	0.1280	1.1900	1.4430	0.1265	1.1570	1.4190	0.1310	0.1285	0.0019	1.4559	0.8462	95.7124
2-15-2023_C183S2	0.30	1.1460	1.3590	0.1065	1.0300	1.2590	0.1145	1.0820	1.2980	0.1080	0.1097	0.0035	3.1661	0.9186	75.2415
2-15-2023_GW4S1	0.30	1.1540	1.2890	0.0675	1.1240	1.2600	0.0680	1.1380	1.2780	0.0700	0.0685	0.0011	1.5768	0.7677	56.2364
2-15-2023_GW4S2	0.30	1.1600	1.2710	0.0555	0.9800	1.1380	0.0790	0.9520	1.1140	0.0810	0.0718	0.0116	16.1182	0.9150	49.4788
2-15-2023_GW5S1	0.30	1.0280	1.2130	0.0925	1.0680	1.2310	0.0815	1.0450	1.2110	0.0830	0.0857	0.0049	5.6855	0.7805	69.1745
2-15-2023_GW5S2	0.30	1.1030	1.2310	0.0640	1.0840	1.2130	0.0645	1.0300	1.1640	0.0670	0.0652	0.0013	2.0138	0.8308	49.4340
2-15-2023_GW6S1	0.30	1.2050	1.4460	0.1205	1.1910	1.4180	0.1135	1.1520	1.4040	0.1260	0.1200	0.0051	4.2628	1.0579	71.4876
2-15-2023_GW6S2	0.30	1.1300	1.3450	0.1075	1.1580	1.3270	0.0845	1.0740	1.2930	0.1095	0.1005	0.0113	11.2867	0.9375	67.5630
BASELINE															
2-23-23_GW1S1	0.30	1.2690	1.5030	0.1170	1.2100	1.4360	0.1130	1.0350	1.3040	0.1345	0.1215	0.0093	7.6842	0.8464	90.4733
2-23-23_GW2S1	0.30	1.1720	1.4450	0.1365	1.2730	1.5120	0.1195	1.2320	1.4880	0.1280	0.1280	0.0069	5.4220	1.0575	76.2858
2-23-23_GW3S1	0.30	1.1710	1.4010	0.1150	1.1770	1.4070	0.1150	1.2000	1.4140	0.1070	0.1123	0.0038	3.3572	0.9563	74.0375
2-23-23_GW4S1	0.30	1.1930	1.4170	0.1120	1.1460	1.3760	0.1150	1.1950	1.3900	0.0975	0.1082	0.0076	7.0643	0.9396	72.5559
2-23-23_GW5S1	0.30	1.3270	1.6830	0.1780	0.9980	1.1340	0.0680	0.9500	1.0970	0.0735	0.0708	0.0028	3.8869	0.4703	94.8170
2-23-23_GW6S1	0.30	1.1450	1.3420	0.0985	1.0540	1.2430	0.0945	1.1160	1.3000	0.0920	0.0950	0.0027	2.8180	0.6681	89.6242
2-23-23_GW1S2	0.30	1.1750	1.3950	0.1100	1.1340	1.3640	0.1150	0.9630	1.1420	0.0895	0.1048	0.0110	10.5241	0.7592	87.0315
2-23-23_GW2S2	0.30	1.2270	1.5420	0.1575	1.1620	1.3850	0.1115	0.7240	0.9100	0.0930	0.1023	0.0093	9.0465	0.9797	65.7771
2-23-23_GW3S2	0.30	1.1460	1.4430	0.1485	1.2400	1.4610	0.1105	1.3240	1.6350	0.1555	0.1520	0.0035	2.3026	0.8588	111.5555
2-23-23_GW4S2	0.30	1.1260	1.4170	0.1455	1.2470	1.4720	0.1125	1.1380	1.4060	0.1340	0.1307	0.0137	10.4670	0.8614	95.6048
2-23-23_GW5S2	0.30	1.1290	1.3440	0.1075	1.0870	1.2580	0.0855	0.9980	1.2080	0.1050	0.0993	0.0098	9.9008	0.7472	83.7837
2-23-23_GW6S2	0.30	0.8770	1.0340	0.0785	0.9610	1.1010	0.0700	0.9910	1.0830	0.0460	0.0743	0.0043	5.7239	0.4631	101.0596

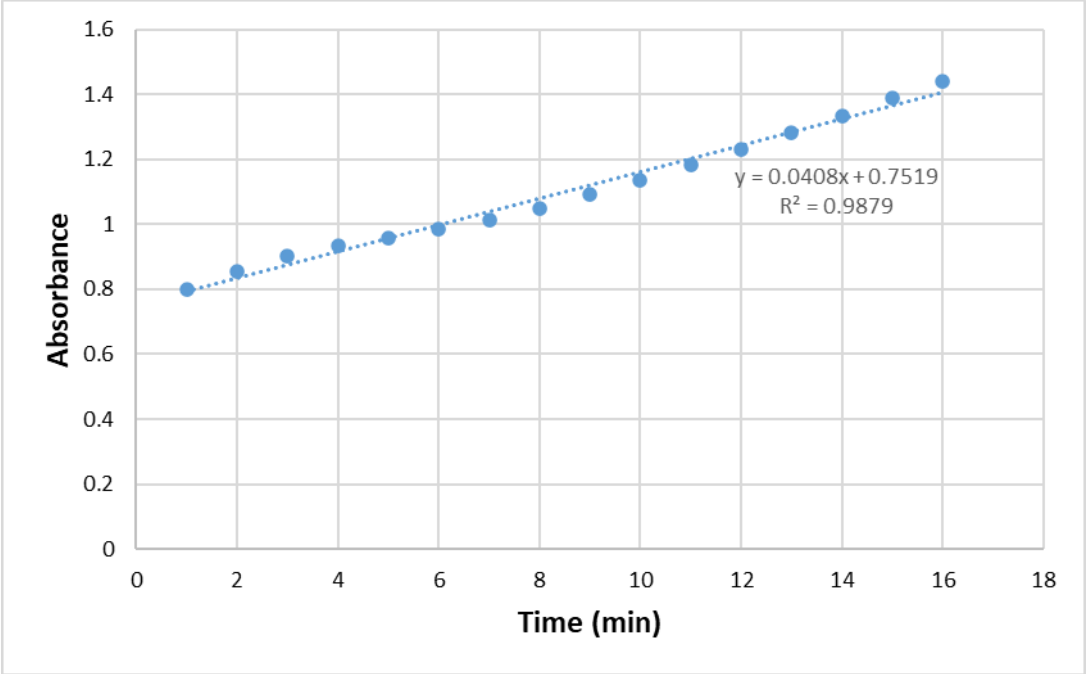

Figure S1: AChE QC standard 2/3/2023 (expected absorbance range: 0.040-0.080 units/min)

Table S13: Average AChE specific activity as percent of baseline data (Figure 14)

Resin	**% Baseline**	**SD**
HLB	98%	18.99%
Glass Wool - HLB	80%	22.29%
C18	94%	24.32%
Glass Wool - C18	70%	15.69%

Table S14: AChE R input (enzyme_activity = specific activity (μmol/min/g protein)

Resin	enzyme_activity
GW_hlb	68.052513
GW_hlb	53.380503
GW_hlb	71.54213
GW_hlb	58.168877
GW_hlb	95.294118
GW_hlb	92.558323
GW_hlb	68.541383
GW_hlb	78.268517
GW_hlb	86.079732
GW_hlb	93.992324
GW_hlb	93.264431
GW_C18	56.236422
GW_C18	49.478808
GW_C18	69.174516
GW_C18	49.434016
GW_C18	71.487635
GW_C18	67.563025
C18	109.48016
C18	73.201349
C18	68.92304
C18	66.702393
C18	95.712376
C18	75.241466
BASELINE	90.473341
BASELINE	76.285833
BASELINE	74.037458
BASELINE	72.555852
BASELINE	94.817017
BASELINE	89.624207
BASELINE	87.03152
BASELINE	65.777091
BASELINE	111.55554
BASELINE	95.604833
BASELINE	83.783699
BASELINE	101.05962

All statistical analysis run in R studio using data in Table S11

Table S15: Two-sample t-test R output comparing HLB run glass wool treatment specific activity to baseline specific activity

```
        Two Sample t-test

data:  enzyme_activity by as.factor(Resin)
t = 2.3507, df = 15, p-value = 0.03283
alternative hypothesis: true difference in means between group BASELINE an
d group GW_hlb is not equal to 0
95 percent confidence interval:
  1.641326 33.551086
sample estimates:
mean in group BASELINE   mean in group GW_hlb
              86.88383               69.28763
```

Table S16: Two-sample t-test R output comparing HLB treatment specific activity to baseline specific activity

```
        Two Sample t-test

data:  enzyme_activity by as.factor(Resin)
t = 0.2326, df = 16, p-value = 0.819
alternative hypothesis: true difference in means between group BASELINE an
d group HLB is not equal to 0
95 percent confidence interval:
 -11.62749  14.49359
sample estimates:
mean in group BASELINE      mean in group HLB
              86.88383               85.45078
```

Table S17: Two-sample t-test R output comparing C18 glass wool treatment specific activity to baseline specific activity

```
        Two Sample t-test

data:  enzyme_activity by as.factor(Resin)
t = 4.2851, df = 16, p-value = 0.000568
alternative hypothesis: true difference in means between group BASELINE an
d group GW_C18 is not equal to 0
95 percent confidence interval:
 13.29992 39.34294
sample estimates:
mean in group BASELINE   mean in group GW_C18
              86.88383               60.56240
```

Table S18: Two-sample t-test R output comparing C18 treatment specific activity to baseline specific activity

```
        Two Sample t-test
data:  enzyme_activity by as.factor(Resin)
t = 0.7352, df = 16, p-value = 0.4729
alternative hypothesis: true difference in means between group BASELINE an
d group C18 is not equal to 0
95 percent confidence interval:
 -10.05827  20.73902
sample estimates:
mean in group BASELINE      mean in group C18
              86.88383               81.54346
```

Appendix D: Ludington Data and Statistical Analysis

Table S19: Average *H. azteca* survival data (± s.d.) and average survival as a percent of baseline (± s.d.) (Figures 5 & 6)

Site	LC Scenario	Chamber	Mean survival (%)	Mean Survival s.d.	Mean Survival as % of Baseline	Mean Surv / Baseline s.d.
E11	LCA	OW	95%	5.80%	110%	11.00%
		SS	75%	24.00%	83%	27.00%
	LCNA	OW	1%	0.00%	0%	0.00%
		SS	1%	0.00%	0%	0.00%
	LCO	OW	90%	12.00%	100%	15.00%
		SS	5%	10.00%	6%	11.00%
REF-E	LCA	OW	90%	8.20%	100%	12.00%
		SS	82%	17.00%	92%	20.00%
	LCNA	OW	70%	16.00%	78%	19.00%
		SS	22%	26.00%	25%	30.00%
	LCO	OW	88%	15.00%	97%	18.00%
		SS	48%	39.00%	53%	43.00%

Table S20: Ludington *H. azteca* survival comparison(s) and beta regression R input

Site	LC_scenario	Chamber	Survival	Percent_Survival	Prop_Survival	Percent_Baseline	Min_DO	Max_Ammonia	Max_pH
E11	LCO	SS	0	0	0.001	0	1.431	0.25	9.29
E11	LCO	SS	0	0	0.001	0	1.431	0.25	9.29
E11	LCO	SS	0	0	0.001	0	1.431	0.25	9.29
E11	LCO	SS	2	20	0.2	22	1.431	0.25	9.29
E11	LCO	OW	10	100	0.999	111	2.317	0.059	9.087
E11	LCO	OW	8	80	0.8	89	2.317	0.059	9.087
E11	LCO	OW	10	100	0.999	111	2.317	0.059	9.087
E11	LCO	OW	8	80	0.8	89	2.317	0.059	9.087
E11	LCA	SS	5	50	0.5	56	5.884	1.4	8.328
E11	LCA	SS	10	100	0.999	111	5.884	1.4	8.328
E11	LCA	SS	6	60	0.6	67	5.884	1.4	8.328
E11	LCA	SS	9	90	0.9	100	5.884	1.4	8.328
E11	LCA	OW	9	90	0.9	100	6.741	0.45	8.684
E11	LCA	OW	9	90	0.9	100	6.741	0.45	8.684
E11	LCA	OW	10	100	0.999	111	6.741	0.45	8.684
E11	LCA	OW	10	100	0.999	111	6.741	0.45	8.684
E11	LCNA	SS	0	0	0.001	0	0	2	8.39
E11	LCNA	SS	0	0	0.001	0	0	2	8.39
E11	LCNA	SS	0	0	0.001	0	0	2	8.39
E11	LCNA	SS	0	0	0.001	0	0	2	8.39
E11	LCNA	OW	0	0	0.001	0	0	0.39	8.621
E11	LCNA	OW	0	0	0.001	0	0	0.39	8.621
E11	LCNA	OW	0	0	0.001	0	0	0.39	8.621
E11	LCNA	OW	0	0	0.001	0	0	0.39	8.621
REF_E	LCO	SS	3	30	0.3	33	2.648	1.8	9.129
REF_E	LCO	SS	8	80	0.8	89	2.648	1.8	9.129
REF_E	LCO	SS	0	0	0.001	0	2.648	1.8	9.129
REF_E	LCO	SS	8	80	0.8	89	2.648	1.8	9.129
REF_E	LCO	OW	8	80	0.8	89	3.264	0.051	8.877
REF_E	LCO	OW	10	100	0.999	111	3.264	0.051	8.877
REF_E	LCO	OW	7	70	0.7	78	3.264	0.051	8.877
REF_E	LCO	OW	10	100	0.999	111	3.264	0.051	8.877
REF_E	LCA	SS	8	80	0.8	89	4.978	0.054	8.524
REF_E	LCA	SS	9	90	0.9	100	4.978	0.054	8.524
REF_E	LCA	SS	10	100	0.999	111	4.978	0.054	8.524
REF_E	LCA	SS	6	60	0.6	67	4.978	0.054	8.524
REF_E	LCA	OW	9	90	0.9	100	5.825	0.069	8.337
REF_E	LCA	OW	10	100	0.999	111	5.825	0.069	8.337
REF_E	LCA	OW	8	80	0.8	89	5.825	0.069	8.337
REF_E	LCA	OW	9	90	0.9	100	5.825	0.069	8.337
REF_E	LCNA	SS	4	40	0.4	44	2.726	0.15	8.544
REF_E	LCNA	SS	0	0	0.001	0	2.726	0.15	8.544
REF_E	LCNA	SS	0	0	0.001	0	2.726	0.15	8.544
REF_E	LCNA	SS	5	50	0.5	56	2.726	0.15	8.544
REF_E	LCNA	OW	5	50	0.5	56	2.771	0.05	8.686
REF_E	LCNA	OW	7	70	0.7	78	2.771	0.05	8.686
REF_E	LCNA	OW	9	90	0.9	100	2.771	0.05	8.686
REF_E	LCNA	OW	7	70	0.7	78	2.771	0.05	8.686

Table S21: R output for Kruskal-Wallis comparing *H. azteca* survival across sites

```
        Kruskal-Wallis rank sum test

data:  Survival by Site
Kruskal-Wallis chi-squared = 1.8099, df = 1, p-value = 0.1785
```

Table S22: R output for Kruskal-Wallis and Dunn's post hoc test comparing *H. azteca* survival across LC scenarios at E-11

```
        Kruskal-Wallis rank sum test

data:  Percent_Survival by LC_scenario
Kruskal-Wallis chi-squared = 13.817, df = 2, p-value = 0.0009994
Dunn (1964) Kruskal-Wallis multiple comparison
  p-values adjusted with the Bonferroni method.

  Comparison         Z      P.unadj       P.adj
1 LCA - LCNA  3.702953 0.0002131043 0.000639313
2  LCA - LCO  1.570950 0.1161943143 0.348582943
3 LCNA - LCO -2.132003 0.0330065775 0.099019732
```

Table S23: R output for Kruskal-Wallis and Dunn's post hoc test comparing *H. azteca* survival across LC scenarios at E-11

```
        Kruskal-Wallis rank sum test

data:  Percent_Survival by as.factor(LC_scenario)
Kruskal-Wallis chi-squared = 7.4117, df = 2, p-value = 0.02458
Dunn (1964) Kruskal-Wallis multiple comparison
  p-values adjusted with the Bonferroni method.

  Comparison         Z     P.unadj      P.adj
1 LCA - LCNA  2.716094 0.006605719 0.01981716
2  LCA - LCO  1.197226 0.231218646 0.69365594
3 LCNA - LCO -1.518868 0.128795659 0.38638698
```

Table S24: R output for Kruskal-Wallis comparing *H. azteca* survival between E-11 and Ref-E LCNA

```
        Kruskal-Wallis rank sum test

data:  Percent_Survival by Site
Kruskal-Wallis chi-squared = 8.4211, df = 1, p-value = 0.003709
```

Table S25: R output for Kruskal-Wallis comparing *H. azteca* survival between E-11 and Ref-E LCA

```
        Kruskal-Wallis rank sum test

data:  Percent_Survival by Site
Kruskal-Wallis chi-squared = 0.10835, df = 1, p-value = 0.742
```

Table S26: R output for Kruskal-Wallis comparing *H. azteca* survival between E-11 and Ref-E LCO

```
        Kruskal-Wallis rank sum test

data:  Percent_Survival by Site
Kruskal-Wallis chi-squared = 0.49512, df = 1, p-value = 0.4817
```

Table S27: R output for Kruskal-Wallis comparing *H. azteca* survival between E-11 and Ref-E OW chambers

```
        Kruskal-Wallis rank sum test

data:  Percent_Survival by Site
Kruskal-Wallis chi-squared = 0.087121, df = 1, p-value = 0.7679
```

Table S28: R output for Kruskal-Wallis comparing *H. azteca* survival between E-11 and Ref-E SS chambers

```
        Kruskal-Wallis rank sum test

data:  Percent_Survival by Site
Kruskal-Wallis chi-squared = 2.1636, df = 1, p-value = 0.1413
```

Table S29: R output for Kruskal-Wallis comparing *H. azteca* OW and SS chamber survival at E-11

```
        Kruskal-Wallis rank sum test

data:  Percent_Survival by Chamber
Kruskal-Wallis chi-squared = 3.1376, df = 1, p-value = 0.07651
```

Table S30: R output for Kruskal-Wallis comparing *H. azteca* OW and SS chamber survival at Ref-E

```
        Kruskal-Wallis rank sum test

data:  Percent_Survival by Chamber
Kruskal-Wallis chi-squared = 4.7895, df = 1, p-value = 0.02863
```

Tabld S31: R output for E-11 beta regression

```
betareg(formula = Prop_Survival ~ Min_DO + Max_Ammonia, data = e11_beta)

Standardized weighted residuals 2:
    Min      1Q  Median      3Q     Max
-1.2671 -0.5425  0.0249  0.2260  2.2043

Coefficients (mean model with logit link):
            Estimate Std. Error z value Pr(>|z|)
(Intercept)  -1.2339     0.5044  -2.446   0.0144 *
Min_DO        0.4468     0.1114   4.011 6.04e-05 ***
Max_Ammonia  -0.3804     0.3457  -1.101   0.2711

Phi coefficients (precision model with identity link):
      Estimate Std. Error z value Pr(>|z|)
(phi)   0.8849     0.2418    3.66 0.000252 ***
---
Signif. codes:  0 '***' 0.001 '**' 0.01 '*' 0.05 '.' 0.1 ' ' 1

Type of estimator: ML (maximum likelihood)
Log-likelihood: 54.86 on 4 Df
Pseudo R-squared: 0.6453
Number of iterations: 31 (BFGS) + 3 (Fisher scoring)
```

Table S32: R output for Ref-E beta regression

```
betareg(formula = Prop_Survival ~ Min_DO + Max_Ammonia, data = refe_beta)

Standardized weighted residuals 2:
    Min      1Q  Median      3Q     Max
-2.4200 -0.4037  0.0087  0.6421  2.0672

Coefficients (mean model with logit link):
            Estimate Std. Error z value Pr(>|z|)
(Intercept)  -1.0496     0.9357  -1.122   0.2620
Min_DO        0.4174     0.2236   1.867   0.0619 .
Max_Ammonia  -0.3600     0.4344  -0.829   0.4073

Phi coefficients (precision model with identity link):
      Estimate Std. Error z value Pr(>|z|)
(phi)   1.0471     0.2545   4.115 3.87e-05 ***
---
Signif. codes:  0 '***' 0.001 '**' 0.01 '*' 0.05 '.' 0.1 ' ' 1

Type of estimator: ML (maximum likelihood)
Log-likelihood: 16.43 on 4 Df
Pseudo R-squared: 0.2109
Number of iterations: 24 (BFGS) + 2 (Fisher scoring)
```

Table S33: Chamber and airstone ammonia (mg/L) data for respective sites and LC scenarios (Figure 8)

Site	LC Scenario	Day	OW Chamber	SS Chamber	Avg Airstone	Airstone s.d.
E-11	*LCNA*	8/2/2022	0.3	0.6	1.85	0.98
		8/3/2022	0.39	1.2	5	1.56
		8/4/2022	0.19	1.7	5.63	1.53
		8/5/2022	0.18	2	9.53	1.68
	LCA	8/2/2022	0.45	1	7.2	3.36
		8/3/2022	0.24	1.3	4.77	0.305
		8/4/2022	0.16	1.3	5.83	3.62
		8/5/2022	0.15	1.4	5.53	0.709
	LCO	8/2/2022	0	0.13	3.13	1.70
		8/3/2022	0.059	0.078	3.03	2.37
		8/4/2022	0	0.12	4.67	0.321
		8/5/2022	0	0.25	3.3	1.34
Ref-E	*LCNA*	8/2/2022	0	0	0.55	0.131
		8/3/2022	0	0	0	0
		8/4/2022	0.05	0.15	0.947	0.260
		8/5/2022	0	0.15	0.787	0.271
	LCA	8/2/2022	0	0.054	0.51	0.111
		8/3/2022	0	0	0	0
		8/4/2022	0.069	0	1.58	0.788
		8/5/2022	0.065	0	1.05	0.175
	LCO	8/2/2022	0	0.086	0.637	0.180
		8/3/2022	0	0	0	0
		8/4/2022	0.051	1.5	1.33	0.462
		8/5/2022	0	1.8	2.8	1.48

Table S34: Ludington ammonia R input (mg/L)

Site	LC_Scenario	Day	Chamber	Ammonia
E11	LCO	1	OW	0
E11	LCO	2	OW	0.059
E11	LCO	3	OW	0
E11	LCO	4	OW	0
E11	LCO	1	SS	0.13
E11	LCO	2	SS	0.078
E11	LCO	3	SS	0.12
E11	LCO	4	SS	0.25
E11	LCA	1	OW	0.45
E11	LCA	2	OW	0.24
E11	LCA	3	OW	0.16

E11	LCA	4	OW	0.15
E11	LCA	1	SS	1
E11	LCA	2	SS	1.3
E11	LCA	3	SS	1.3
E11	LCA	4	SS	1.4
E11	LCNA	1	OW	0.3
E11	LCNA	2	OW	0.39
E11	LCNA	3	OW	0.19
E11	LCNA	4	OW	0.18
E11	LCNA	1	SS	0.6
E11	LCNA	2	SS	1.2
E11	LCNA	3	SS	1.7
E11	LCNA	4	SS	2
REF_E	LCO	1	OW	0
REF_E	LCO	3	OW	0.051
REF_E	LCO	4	OW	0
REF_E	LCO	1	SS	0.086
REF_E	LCO	3	SS	1.5
REF_E	LCO	4	SS	1.8
REF_E	LCA	1	OW	0
REF_E	LCA	3	OW	0.069
REF_E	LCA	4	OW	0.065
REF_E	LCA	1	SS	0.054
REF_E	LCA	3	SS	0
REF_E	LCA	4	SS	0
REF_E	LCNA	1	OW	0
REF_E	LCNA	3	OW	0.05
REF_E	LCNA	4	OW	0
REF_E	LCNA	1	SS	0
REF_E	LCNA	3	SS	0.15
REF_E	LCNA	4	SS	0.15
E11	LCA	1	Airstone	6
E11	LCA	1	Airstone	4.6
E11	LCA	2	Airstone	4.5
E11	LCA	2	Airstone	5.1
E11	LCA	2	Airstone	4.7
E11	LCA	3	Airstone	3.4
E11	LCA	3	Airstone	10
E11	LCA	3	Airstone	4.1
E11	LCA	4	Airstone	6.3
E11	LCA	4	Airstone	4.9
E11	LCA	4	Airstone	5.4
E11	LCNA	1	Airstone	0.95
E11	LCNA	1	Airstone	1.7

E11	LCNA	1	Airstone	2.9
E11	LCNA	2	Airstone	4.2
E11	LCNA	2	Airstone	4
E11	LCNA	2	Airstone	6.8
E11	LCNA	3	Airstone	4.8
E11	LCNA	3	Airstone	7.4
E11	LCNA	3	Airstone	4.7
E11	LCNA	4	Airstone	11
E11	LCNA	4	Airstone	9.9
E11	LCNA	4	Airstone	7.7
E11	LCO	1	Airstone	5.1
E11	LCO	1	Airstone	2.1
E11	LCO	1	Airstone	2.2
E11	LCO	2	Airstone	5.5
E11	LCO	2	Airstone	0.78
E11	LCO	2	Airstone	2.8
E11	LCO	3	Airstone	4.3
E11	LCO	3	Airstone	4.8
E11	LCO	3	Airstone	4.9
E11	LCO	4	Airstone	1.8
E11	LCO	4	Airstone	4.4
E11	LCO	4	Airstone	3.7
REF_E	LCA	1	Airstone	0.39
REF_E	LCA	1	Airstone	0.53
REF_E	LCA	1	Airstone	0.61
REF_E	LCA	3	Airstone	1.5
REF_E	LCA	3	Airstone	2.4
REF_E	LCA	3	Airstone	0.83
REF_E	LCA	4	Airstone	0.86
REF_E	LCA	4	Airstone	1.2
REF_E	LCA	4	Airstone	1.1
REF_E	LCNA	1	Airstone	0.41
REF_E	LCNA	1	Airstone	0.67
REF_E	LCNA	1	Airstone	0.56
REF_E	LCNA	3	Airstone	0.96
REF_E	LCNA	3	Airstone	1.2
REF_E	LCNA	3	Airstone	0.68
REF_E	LCNA	4	Airstone	0.63
REF_E	LCNA	4	Airstone	0.63
REF_E	LCNA	4	Airstone	1.1
REF_E	LCO	1	Airstone	0.46
REF_E	LCO	1	Airstone	0.82
REF_E	LCO	1	Airstone	0.63
REF_E	LCO	3	Airstone	1.6

REF_E	LCO	3	Airstone	1.6
REF_E	LCO	3	Airstone	0.8
REF_E	LCO	4	Airstone	4.5
REF_E	LCO	4	Airstone	2.1
REF_E	LCO	4	Airstone	1.8

Table S35: R output for Kruskal-Wallis comparing OW to SS chamber ammonia across all sites and LC scenarios

```
        Kruskal-Wallis rank sum test

data:  Ammonia by Chamber
Kruskal-Wallis chi-squared = 7.588, df = 1, p-value = 0.005876
```

Table S36: R output for Kruskal-Wallis comparing chamber ammonia between sites

```
Kruskal-Wallis rank sum test

data:  Ammonia by Site
Kruskal-Wallis chi-squared = 9.7935, df = 1, p-value = 0.001751
```

Table S37: R output for Kruskal-Wallis comparing OW chamber ammonia between sites

```
        Kruskal-Wallis rank sum test

data:  Ammonia by Site
Kruskal-Wallis chi-squared = 5.6424, df = 1, p-value = 0.01753
```

Table S38: R output for Kruskal-Wallis comparing SS chamber ammonia between sites

```
        Kruskal-Wallis rank sum test

data:  Ammonia by Site
Kruskal-Wallis chi-squared = 3.4275, df = 1, p-value = 0.06412
```

Table S39: R output for Kruskal-Wallis and Dunn's post hoc test comparing chamber ammonia across E-11 LC scenarios

```
Kruskal-Wallis rank sum test

data:  Ammonia by LC_Scenario
Kruskal-Wallis chi-squared = 13.144, df = 2, p-value = 0.001399

Dunn (1964) Kruskal-Wallis multiple comparison
  p-values adjusted with the Bonferroni method.

  Comparison          Z     P.unadj       P.adj
1 LCA - LCNA -0.2477568 0.804322565 1.000000000
2  LCA - LCO  3.0084757 0.002625618 0.007876854
3 LCNA - LCO  3.2562325 0.001129013 0.003387038
```

Table S40: R output for Kruskal-Wallis comparing chamber ammonia across Ref-E LC scenarios

```
        Kruskal-Wallis rank sum test

data:  Ammonia by LC_Scenario
Kruskal-Wallis chi-squared = 1.2147, df = 2, p-value = 0.5448
```

Table S41: R output for Kruskal-Wallis comparing E-11 OW and SS chamber ammonia

```
        Kruskal-Wallis rank sum test

data:  Ammonia by Chamber
Kruskal-Wallis chi-squared = 6.7647, df = 1, p-value = 0.009298
```

Table S42: R output for Kruskal-Wallis comparing Ref-E OW and SS chamber ammonia

```
        Kruskal-Wallis rank sum test

data:  Ammonia by Chamber
Kruskal-Wallis chi-squared = 3.0855, df = 1, p-value = 0.07899
```

Table S43: R output for Kruskal-Wallis comparing Ref-E and E-11 LCA combined chamber ammonia

```
        Kruskal-Wallis rank sum test

data:  Ammonia by Site
Kruskal-Wallis chi-squared = 9.7067, df = 1, p-value = 0.001836
```

Table S44: R output for Kruskal-Wallis comparing Ref-E and E-11 LCNA combined chamber ammonia

```
        Kruskal-Wallis rank sum test

data:  Ammonia by Site
Kruskal-Wallis chi-squared = 9.7067, df = 1, p-value = 0.001836
```

Table S45: R output for Kruskal-Wallis comparing Ref-E and E-11 LCO combined chamber ammonia

```
        Kruskal-Wallis rank sum test

data:  Ammonia by Site
Kruskal-Wallis chi-squared = 0.1569, df = 1, p-value = 0.692
```

Table S46: R output for Kruskal-Wallis comparing Ref-E and E-11 airstone ammonia

```
        Kruskal-Wallis rank sum test

data:  Ammonia by Site
Kruskal-Wallis chi-squared = 36.078, df = 1, p-value = 1.896e-09
```

Table S47: R output for Kruskal-Wallis comparing airstone ammonia across E-11 LC scenarios

```
Kruskal-Wallis rank sum test

data:  Ammonia by LC_Scenario
Kruskal-Wallis chi-squared = 4.4455, df = 2, p-value = 0.1083
```

Table S48: R output for Kruskal-Wallis comparing airstone ammonia across Ref-E LC scenarios

```
        Kruskal-Wallis rank sum test

data:  Ammonia by LC_Scenario
Kruskal-Wallis chi-squared = 3.192, df = 2, p-value = 0.2027
```

Table S49: R output for Kruskal-Wallis and Dunn's post hoc test comparing E-11 OW chamber, SS chamber, and airstone ammonia

```
        Kruskal-Wallis rank sum test

data:  Ammonia by Chamber
Kruskal-Wallis chi-squared = 40.379, df = 2, p-value = 1.706e-09
Dunn (1964) Kruskal-Wallis multiple comparison
  p-values adjusted with the Bonferroni method.

     Comparison         Z      P.unadj        P.adj
1 Airstone - OW  5.705822 1.157832e-08 3.473495e-08
2 Airstone - SS  4.160935 3.169468e-05 9.508404e-05
3       OW - SS -1.265891 2.055520e-01 6.166559e-01
```

Table S50: R output for Kruskal-Wallis and Dunn's post hoc test comparing Ref-E OW chamber, SS chamber, and airstone ammonia

```
        Kruskal-Wallis rank sum test

data:  Ammonia by Chamber
Kruskal-Wallis chi-squared = 23.568, df = 2, p-value = 7.625e-06
Dunn (1964) Kruskal-Wallis multiple comparison
  p-values adjusted with the Bonferroni method.

     Comparison         Z      P.unadj        P.adj
1 Airstone - OW  4.560203 5.110415e-06 1.533125e-05
2 Airstone - SS  2.752290 5.918005e-03 1.775401e-02
3       OW - SS -1.476155 1.399024e-01 4.197071e-01
```

Table S51: Average chloride and TDS (mg/L) for E-11 and Ref-E LC scenarios (Figure 12)

Site	LC Scenario	Chloride	Chloride s.d.	TDS	TDS s.d.
E11	LCO	23	3.1	220	17
	LCA	39	5.3	240	25
	LCNA	47	6.6	230	76
REF-E	LCO	23	1.5	190	10
	LCA	23	0.58	170	29
	LCNA	23	0.5	180	26

Table S52: R input for chloride and TDS site and LC comparisons

Site	LC_Scenario	Sampling_Method	Day	Ammonia	Chloride	TDS
E11	LCO	SW	1	0.081	23	210
E11	LCO	SW	2	0.14	26	240
E11	LCO	SW	3	0	19	210
E11	LCO	SW	4	0.13	25	240
E11	LCA	SW	1	0.42	48	260
E11	LCA	SW	2	0.24	37	250
E11	LCA	SW	3	0.21	35	200
REF_E	LCA	SW	3	0.22	36	250
REF_E	LCA	SW	4	0.29	37	260
REF_E	LCNA	SW	1	0.32	45	250
REF_E	LCNA	SW	2	0.38	42	100
REF_E	LCNA	SW	2	0.39	42	260
REF_E	LCNA	SW	3	0.49	47	270
E11	LCNA	SW	4	0.61	58	290
E11	LCO	SW	1	0	25	180
E11	LCO	SW	3	0.087	22	190
E11	LCO	SW	4	0	23	200
E11	LCA	SW	1	0.079	24	150
E11	LCA	SW	3	0.072	23	200
E11	LCA	SW	4	0.082	23	150
E11	LCNA	SW	1	0	24	160
E11	LCNA	SW	3	0.067	23	210
E11	LCNA	SW	4	0.13	23	160
E11	LCNA	SW	4	0.14	23	200

Table S53: R output for Kruskal-Wallis comparing E-11 and Ref-E chloride concentrations (mg/L)

```
        Kruskal-Wallis rank sum test

data:  Site by Chloride
Kruskal-Wallis chi-squared = 20.444, df = 13, p-value = 0.08467
```

Table S54 R output for Kruskal-Wallis comparing E-11 and Ref-E TDS concentrations (mg/L)

```
        Kruskal-Wallis rank sum test

data:  Site by TDS
Kruskal-Wallis chi-squared = 16.185, df = 11, p-value = 0.1344
```